Chapter 3: Results

3.1 Conservation and domain structure of LepA

The *lepA* gene is the first cistron of a bi-cistronic operon. The second cistron is the leader peptidase or *lep* gene encoding the signal peptidase Lep (March and Inouye, 1985a) - an integral membrane protein that is inserted into the inner membrane and cuts off the N-terminal signal (leader peptide) from secreted and periplasmic proteins (Zwizinski and Wickner, 1980). Dibb and Wolfe reported that a LepA knock-out in *E. coli* has no phenotype under the various growth conditions tested (Dibb and Wolfe, 1986). Curiously, these null-results contrast with the fact that LepA is one of the most conserved proteins on this planet (amino acid identity 55-68%), more conserved even than other essential bacterial translation factors such as initiation factor IF3 or guanine exchange factor EF-Ts (Table 3.1).

Table 3.1 **Conservation of bacterial factors**

Protein	NCBI GenPept ID (gi) of *E.coli* sequence	Range of identity (in %) with bacterial orthologs		
EF-Tu	1790412	70.3	-	82.0
EF-G	62288080	58.3	-	70.3
LepA	16130494	54.6	-	67.7
IF-2	16131060	34.5	-	49.2
IF-3	16129674	42.8	-	69.4
EF-Ts	1786366	32.5	-	49.5

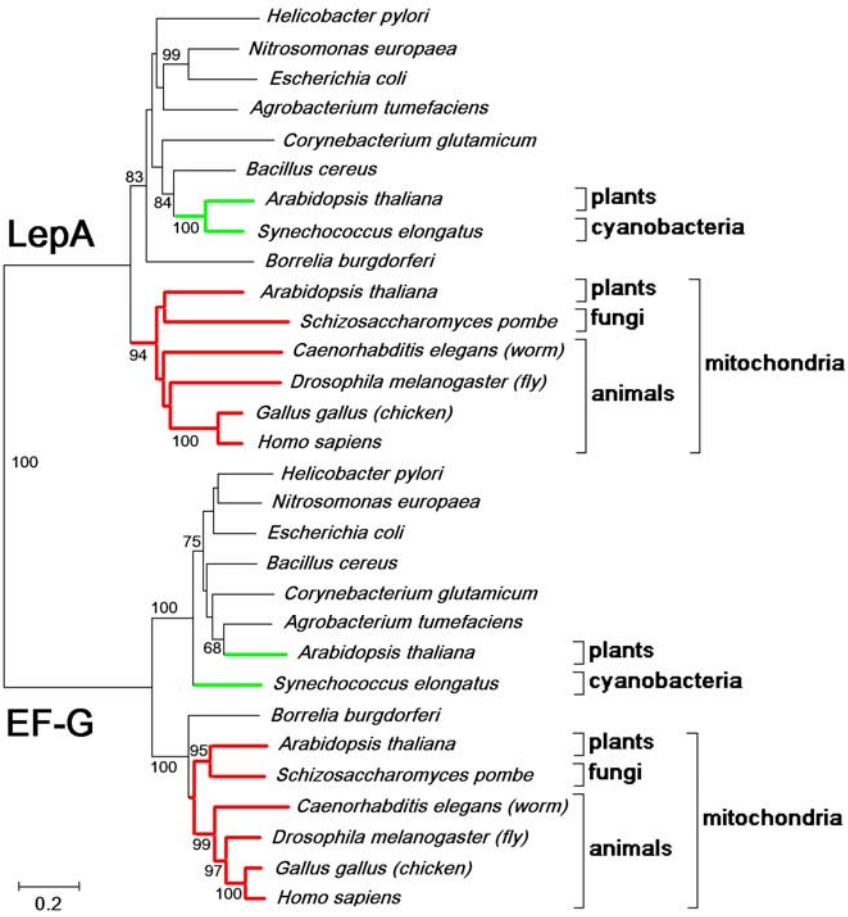

Figure 3.1_1 **Phylogenetic analysis of LepA and EF-G**

Database searches revealed that LepA is also present in the obligatory parasite *Mycoplasma*, which has a minimized bacterial genome containing only ~500 genes; *Rickettsia*, the smallest free-living bacteria. LepA orthologs can be found in all bacteria and nearly all mitochondria. It is only missing in eukaryotes that have lost mitochondria like *Giardia lamblia* or *Encephalitozoon cuniculi*. In all plants with completely sequenced genomes (rice, mouse-ear cress, and red algae) we found two forms of LepA. Whereas one form branches with other mitochondria LepA sequences in our phylogenetic analysis, the second form branched with cyanobacterial orthologs, suggesting its subcellular targeting to chloroplasts in plants (see Figure 3.1_1 and Figure 3.5.1). This suggests that LepA is essential for bacteria, mitochondria and plastids. We note that LepA phylogeny largely reflects the canonical species phylogeny and shows no signs of inter-domain horizontal gene transfer (HGT). With respect to this aspect it behaves rather like a ribosomal protein and not like tRNA synthetases that frequently undergo HGT.

Figure 3.1_1 shows an unrooted NJ (Neighbor Joining algorithm) tree of EF-G and LepA proteins enables reciprocal rooting of each subfamily. Branch lengths reflect the estimated amino acid substitutions per 100 sites (see scale bar). Numbers on internal

branches indicate statistical support of clades based on 1000 bootstrap samples. Note that the total branch lengths of both GTPase families are comparable. In both families mitochondrial eukaryotic proteins are monophyletic. Fly EF-G and LepA proteins branch with their animal orthologs (confirmation of the coelomata hypothesis). A prospective secondary LepA protein of Arabidopsis branches with chloroplasts. There are no signs of inter-domain lateral gene transfer in the LepA family.

E. coli LepA is a polypeptide of 599 amino acid residues with a molecular weight of 67 kDa. The amino acid sequence of LepA indicates that it is a G-protein. As well as having high conservation with EF-G, LepA also exhibits a conspicuous similarity in terms of the domain structure with EF-G, namely containing EF-G domains I to V, with the exception that domain IV is absent (see Figure 3.1_2). The enormous conservation encompasses all five domains of LepA, the first four being strongly related to the EF-G domains I, II, III and V, and the last CTD is unique. This domain arrangement of LepA is found in bacteria and mitochondria from yeast to human (Figure 3.1_2). Due to the high conservation between EF-G and LepA, it is possible to generate a homology model for LepA based on the known EF-G structure (PDB1WDT). As seen in Figure 3.1_3 LepA lacks the G' subdomain of EF-G as well as the complete domain IV. Since the majority of overproduced LepA (March and Inouye, 1985b) is found in the periplasmic membrane, one might speculate that this is related to the LepA specific CTD.

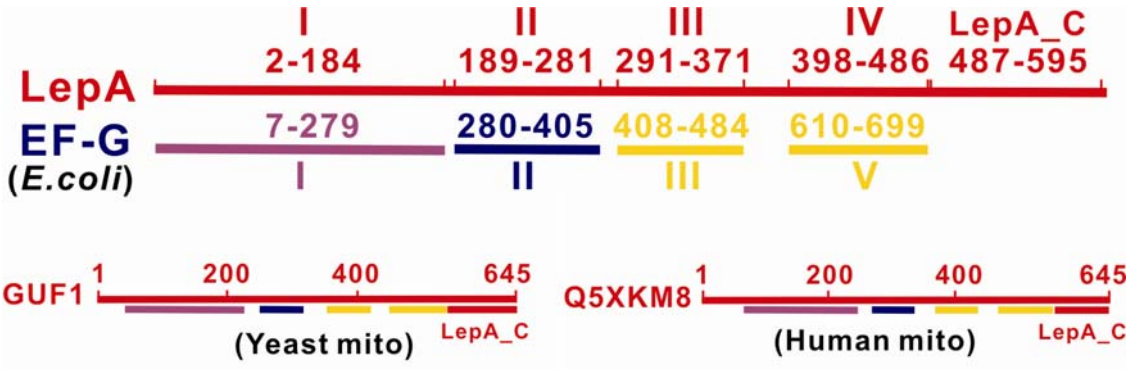

Figure 3.1_2 **Domain structures of LepA and orthologs in comparison with EF-G**

LepA (*E. coli*) and orthologs Guf1 (yeast mitochondria) and Q5XKMB (human mitochondria) in red, corresponding EF-G domains in different colors. LepA has five potential structural domains (I, II, III, IV and LepA_C) according to the amino acid sequence (2-595), which have high consensus with *E. coli* EF-G domains I (purple), II (blue), III and V (yellow).

EF-G is a structural mimic of the ternary complex aa-tRNA•EF-Tu•GTP (Nissen et al., 2000) and according to this mimicry domain IV corresponds to the anticodon loop region of the ternary complex that interacts with the decoding center at the A site of the ribosome (Figure 3.1_3). Removing domain IV of EF-G destroys the translocation activity of EF-G (Martemyanov and Gudkov, 1999).

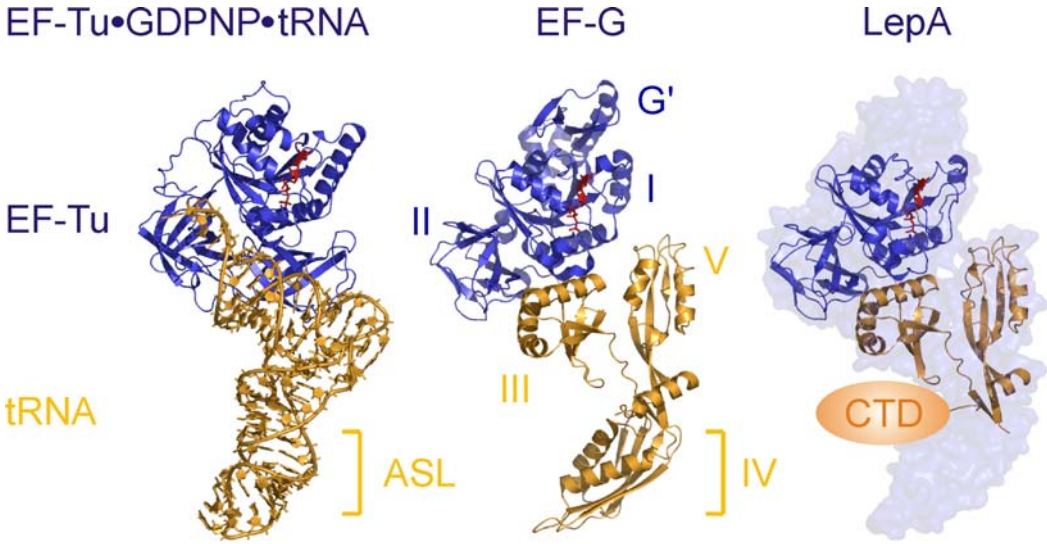

Figure 3.1_3 **Comparison of the structure of the ternary complex aa-tRNA•EF-Tu•GTP with that of EF-G and LepA**
According to (Andersen et al., 2003), the domains are indicated with roman numbers except the G' domain of EF-G. Note that the EF-G domain IV corresponds to the anticodon stem-loop (ASL) of the aa-tRNA within the ternary complex. When fitting the sequence of LepA into the known tertiary structure of EF-G, LepA is found lacks the G' domain and domain IV of EF-G and has in addition a CTD domain.

Here we demonstrate that LepA is a third essential bacterial elongation factor with a novel function in translation that rationalizes the high conservation of this factor. We find that a knock-out of the *lepA* gene is lethal at higher ionic strength and that overexpression of LepA protein is toxic to the cell. LepA is a G protein with an uncoupled ribosome dependent GTPase activity rivaling that of EF-G in terms of turn-over rate. Our analysis reveals a surprising and unique function for LepA, namely to induce "back-translocation" of tRNAs on the ribosome. Collectively, our results suggest that LepA recognizes ribosomes stuck with mis-translocated tRNAs, induces a back-translocation, and enabling efficient synthesis of fully active proteins in bacterial lysates.

3.2 In vivo *analyses of LepA*

3.2.1 Effects of LepA over-expression

3.2.1.1 Construction of LepA over-expression vector and LepA purification

E. coli. lepA gene was cloned from genomic DNA using PCR primers that introduce NdeI and BamHI restriction sites for cloning into the expression vector pET14b (Novagen). The cultures of *E. coli* BL21-DE3 strain or the same strain but transformed with either pET or pET_*lepA* were grown overnight with 150 rpm shaking at 37 °C. Cells were diluted 1:200 and grown for 2–3 h at 37 °C. When the optical density reached an A_{580} of ~0.4, the cells were induced with 1mM IPTG. The cells were harvest at A_{580} of ~0.7. The protein was purified by Ni-NTA column.

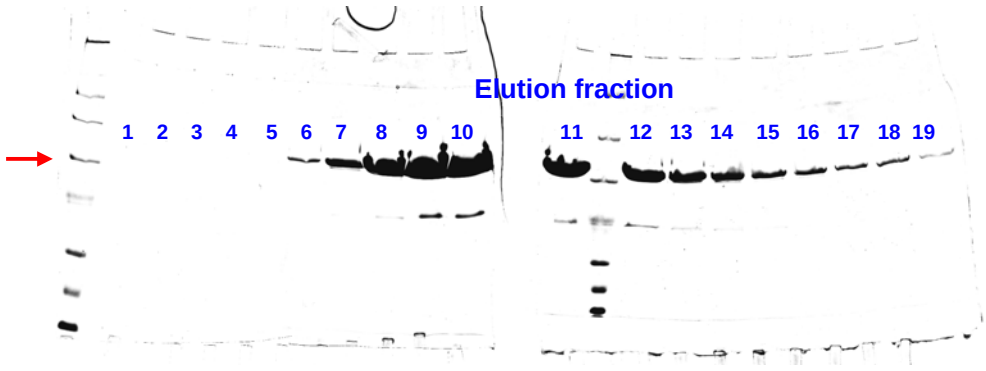

Figure 3.2.1.1 **Purification of over-expressed LepA**
The protein marker on the left with a red arrow is 66 kDa. The LepA protein with 7x His tag on the N-terminus has a molecular weight of 68 kDa, which appeared in elution fraction Nr. 6 with a high purity.

3.2.1.2 LepA over-expression inhibits cell growth

The *E. coli lepA* gene was cloned behind an IPTG inducible lac promoter and transformed into a standard *E. coli* BL21 strain. Even without induction, we observe a prolonged lag phase before growth, a normal generation time in the log phase, but an early entry into the stationary phase compared to the control strain BL21 containing an empty vector. SDS-PAGE analysis reveals leaky expression of exogenous LepA in addition to the chromosomal endogenous LepA, explaining the modest affect on growth.

Consistently, the induction of LepA expression by addition of 1mM IPTG severely affected growth, reducing the rate and promoting entry into stationary phase at much lower cell density (Figure 3.2.1.2). These results demonstrate that overexpression of LepA is toxic to the cells.

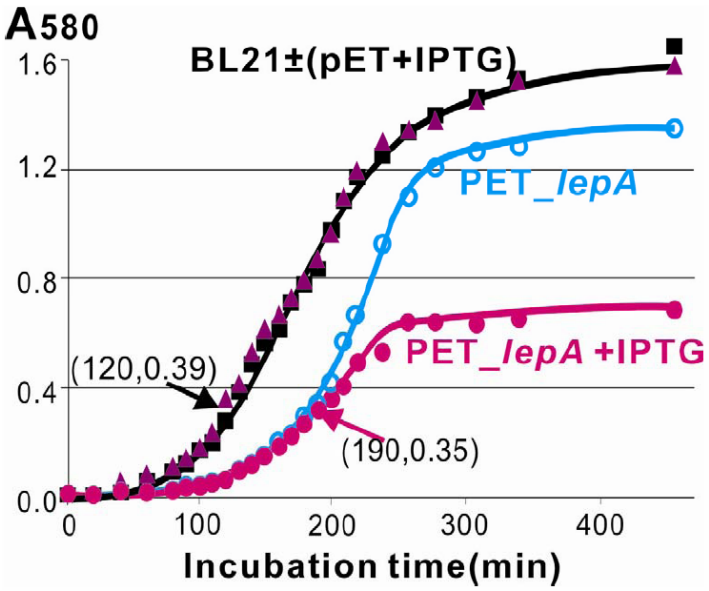

Figure 3.2.1.2 **Overexpression of LepA blocks growth**
The strain BL21 DE3 containing the plasmid (pET+lepA) stops growth soon after IPTG induction (closed circles). Without IPTG induction (open circles) growth is mildly affected due to the leakiness of the (pET+lepA) plasmid as compared to the controls BL21 DE3 without and with the empty pET plasmid (squares and triangles, respectively). The arrows indicate the addition of IPTG (1 mM).

3.2.2 Effects of lepA knock-out

3.2.2.1 Wild type and *lepA* knock-out strain in LB medium

In 1986, Dibb und Wolf reported that an *E. coli* strain with the chromosomally disrupted *lepA* gene was viable (Dibb and Wolfe, 1986). Here similar experiments have been performed. Although the *lepA* knock-out strain is viable, the generation time of this knock-out strain is already retarded (from 30 min to 40 min) even in rich LB medium, and the growth turned into the stationary phase at A_{580} ~0.8. Furthermore, this effect can be reproduced after 10-fold dilution of cells that have reached the stationary phase (Figure 3.2.2.1).

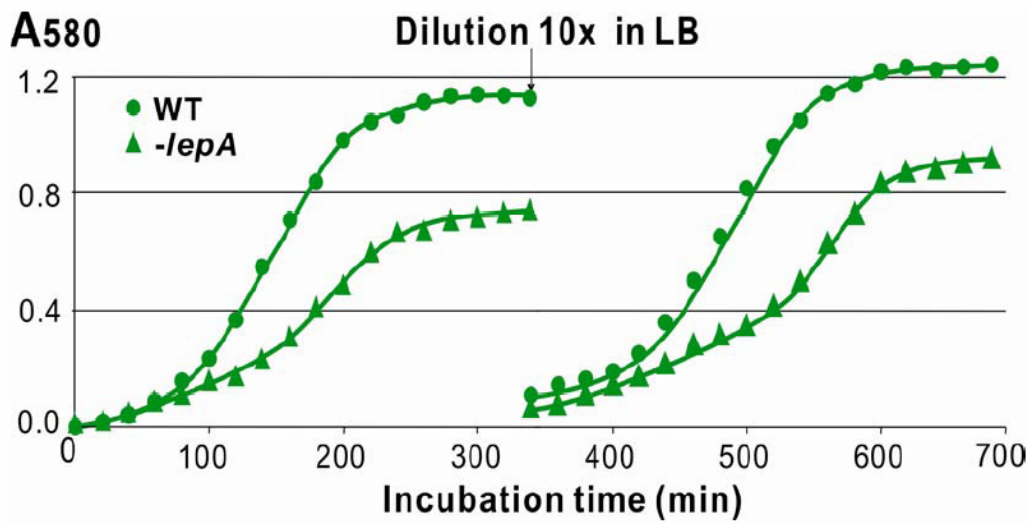

Sample	Growth Rate (min)	After 7hs (A_{580})
WT in LB	**30**	**1.18**
-lepA in LB	**40**	**0.75**

Figure 3.2.2.1 **WT or *lepA* knock-out strain in LB**

3.2.2.2 Wild type and *lepA* knock-out strain in LB medium +K^+

When the growth of the strains with and without the *lepA* gene again was performed in LB medium, but now in the presence of 100-500 mM K^+, the wild-type strain grew normally after a short adaptation phase and maintained wild type -like growth after a ten-fold dilution. In striking contrast, cells bearing an inactivated *lepA* gene exhibited a serious growth defect in the presence of the high potassium (≥200 mM), growth completely ceased after 5 hours, furthermore it did not resume following ten-fold dilution (Figure 3.2.2.2).

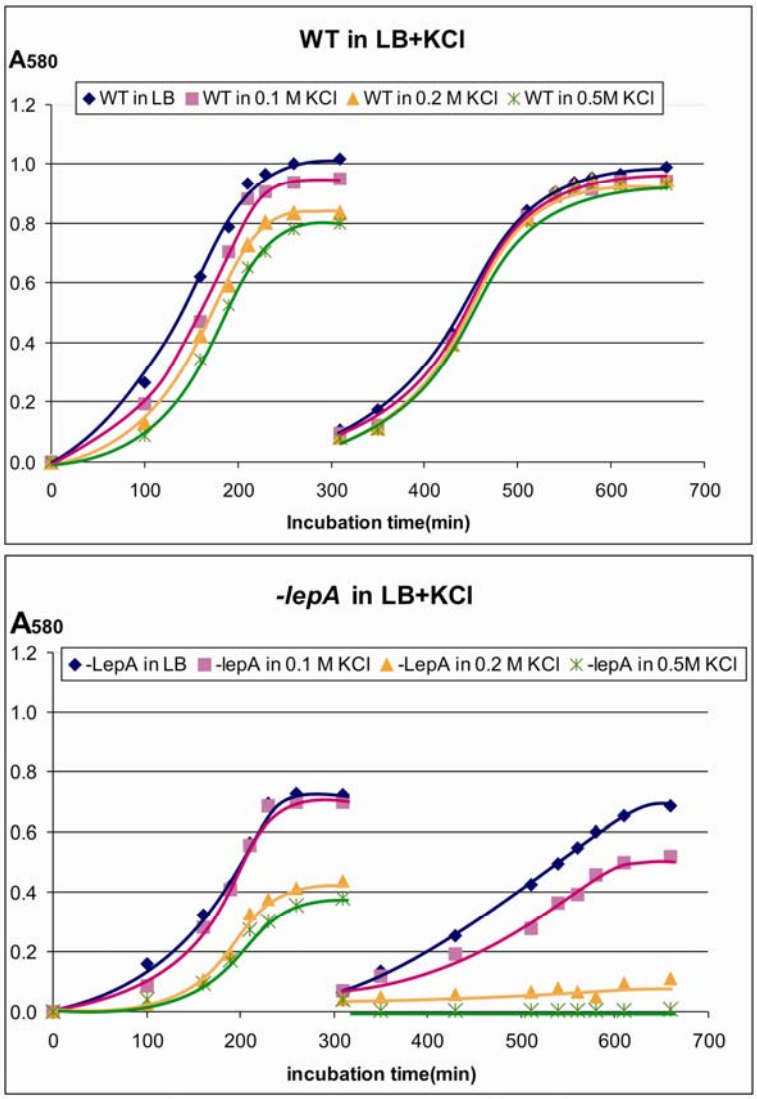

Figure 3.2.2.2 **WT or *lepA* knock-out strain in LB+KCl**

3.2.2.3 Wild type and *lepA* knock-out strain in LB medium plus Mg^{2+}

In this section we test growth in the presence of 10-100 mM Mg^{2+}. The wild-type strain grew normally after a short adaptation phase and maintained wild-type-like growth patterns after a ten-fold dilution. In striking contrast, cells bearing an inactivated *lepA* gene exhibited a serious growth defect in the presence of the high magnesium (100 mM), growth completely ceased after 5 hours, furthermore it did not resume following ten-fold dilution (Figure 3.2.2.3). These results and those of the preceding section indicate that LepA is essential for cell viability under conditions of high ionic strength.

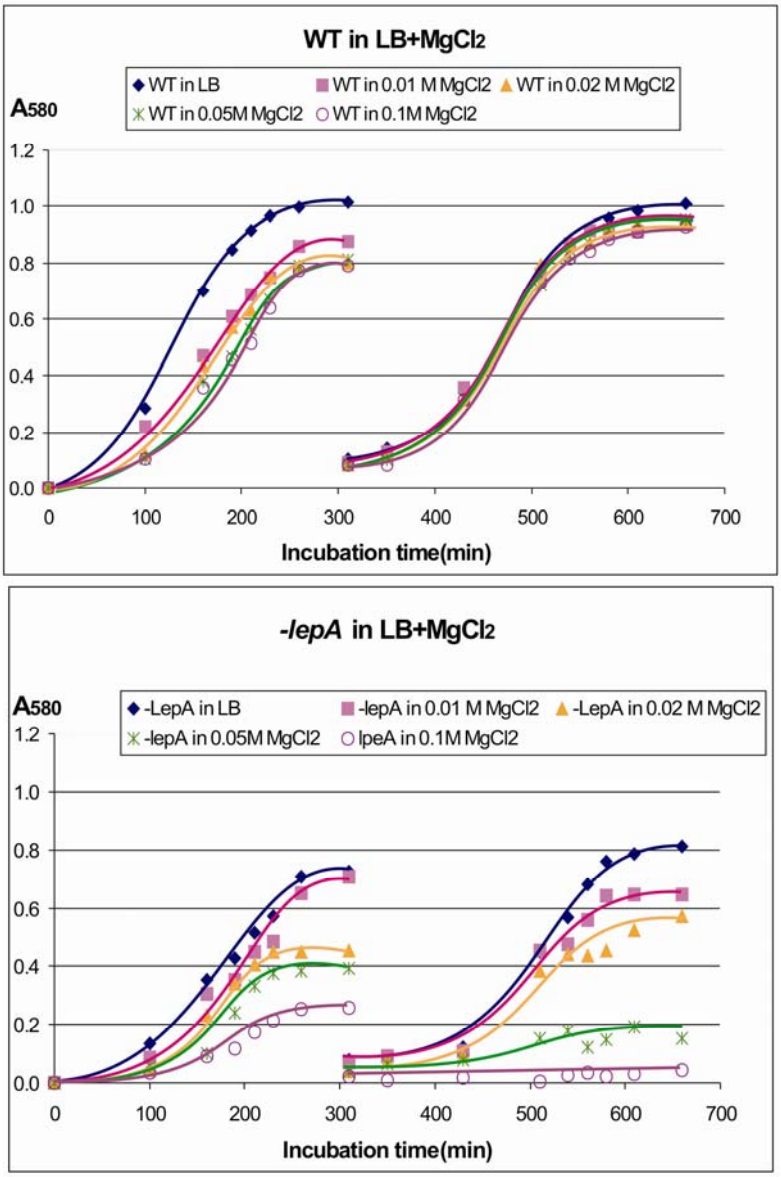

Figure 3.2.2.3 **WT or l*epA* knock-out strain in LB+$MgCl_2$**

3.2.3 LepA distribution in the cell (membrane versus cytoplasmic fraction)

3.2.3.1 LepA distribution under normal condition (LB medium)

We tested the distribution of LepA in the membrane and cytoplasm fractions in a wild type *E. coli* strain and compared it with the amounts of ribosome present in these fractions. The presence of LepA was monitored using a polyclonal antibody raised against *E. coli* LepA and that of the ribosomes using antibodies to the large subunit

ribosomal protein L2. Defined amounts of LepA and ribosomes were applied to the SDS-PAGE gels, which allowed the relative and absolute amounts of LepA and ribosomes to be assessed (table 3.2.3.1). We found 90% of the total cellular LepA to be present in the membrane fraction, whereas only 10% was found in the cytoplasm. Astonishingly, ribosomes were equally distributed between both fractions, leading to a (0.3-0.4):1 ratio of LepA:70S ribosomes in the cell. However, in the cytoplasmic fraction the amount of LepA leads to a ratio of 0.1:1, i.e. one LepA molecule per 10 ribosomes.

Table 3.2.3.1 **Distribution of LepA in wild type cells under normal condition**

	Controls			S30 frac.				membrane frac.			
Anti-LepA											
LepA (pmol)	0.2	0.1	0.05	0.14	0.07	0.03	(0.01)	1.24	0.62	0.37	(0.11)
				9.3±1.5% of LepA				90.7±1.5% of LepA			
Anti-L2											
70S (pmol)	0.5	0.2	0.1	1.72	0.76	0.39	(0.13)	1.24	0.80	0.50	(0.24)
				50.2±7.3% of 70S				49.8±7.3% of 70S			
LepA/70S				**0.08±0.008**				**0.84±0.14**			

3.2.3.2 LepA distribution under high ionic condition

Since the LepA protein is essential at high ionic condition, the distribution under such condition will be of great interest. Here, wild type cells grown in LB in the presence of 100 mM $MgCl_2$ were analyzed with the same method as described in the preceding section. Surprisingly, the results (table 3.2.3.2) turned out to be totally different as seen one before, namely significantly more LepA was found in the cytoplasm (S30) fraction. Instead of 10% about 50% of the total cellular LepA was found in the cytoplasmic fraction. About 60% of the ribosomes were located in the membrane. The total cellular molar ratio of LepA to 70S is 0.5:1 (in the cytoplasmic fraction the ratio is ~0.6:1 and in the membrane fraction is ~0.4:1).

Table 3.2.3.2 **Distribution of LepA in wild type cells under high ionic condition**

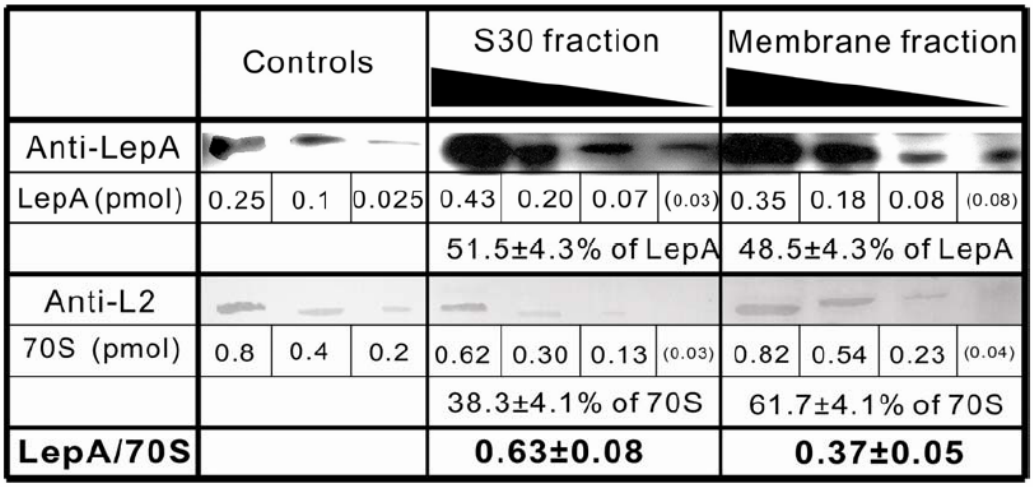

	Controls			S30 fraction				Membrane fraction			
Anti-LepA											
LepA (pmol)	0.25	0.1	0.025	0.43	0.20	0.07	(0.03)	0.35	0.18	0.08	(0.08)
				51.5±4.3% of LepA				48.5±4.3% of LepA			
Anti-L2											
70S (pmol)	0.8	0.4	0.2	0.62	0.30	0.13	(0.03)	0.82	0.54	0.23	(0.04)
				38.3±4.1% of 70S				61.7±4.1% of 70S			
LepA/70S				**0.63±0.08**				**0.37±0.05**			

3.3 In vitro *analyses of LepA*

Knock-out of *lepA* gene is lethal at high ionic condition. Under ionic stress the majority of LepA was found in the cytoplasm, in contrast to normal conditions. What LepA does to help the cells to overcome the ionic stress?

We have seen from our computational analysis, LepA is known as a universal bacterial GTPases that might regulate ribosome function. First we will test its binding to the ribosome before we will analyze its GTPase activity and its influence to other ribosomal functions.

3.3.1 LepA binding assay

3.3.1.1 Saturating binding of LepA with re-associated 70S

LepA is a GTPase, accordingly the binding of LepA in the presence of GTP or non-hydrolysable analogue GDPNP to re-associated *E. coli* 70S ribosome was carried out. Figure 3.3.1.1_1 shows that LepA can bind to re-associated 70S in the presence of GTP, similar to an elongation factor (EF-G•GTP, or aa-tRNA•EF-Tu•GTP). With non-hydrolysable analogue GDPNP LepA bound better (red arrow).

1	2	3	4	5	6	7	8	9	10	11	12	13	14	15	16
M	70S			70S+LepA			70S+LepA+ GTP			70S+LepA+ GDPNP			LepA		
	Pre	Su	Pe	Pre	Su	Pe	Pre	Su	Pe	Pre	Su	Pe	Pre	Su	Pe

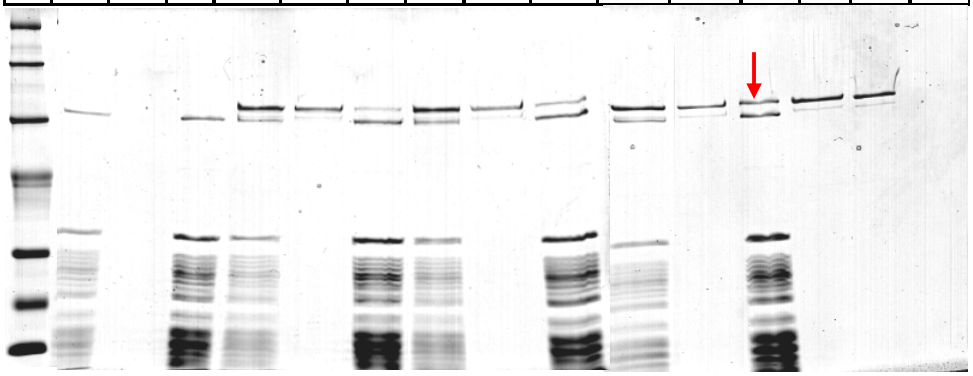

Figure 3.3.1.1_1 **Binding of LepA with *E. coli* re-associated 70S ribosome**

E. coli LepA (red arrow) in GTP or GDPNP form was incubated with complete *E. coli* 70S. After incubation the mix (Pre) was centrifuged through sucrose cushion (50 µl 10% sucrose, sample size 100 µl) and separated into supernatant (Su, about upper 70 µl) and pellet (Pe).

in a saturation curve with LepA with GDPNP the occupancy of LepA to 70S leveled off at ~50%. This could be confirmed even at a LepA excess over ribosomes of 10.1: the binding (ν) was still 0.5 (Figure 3.3.1.1_2).

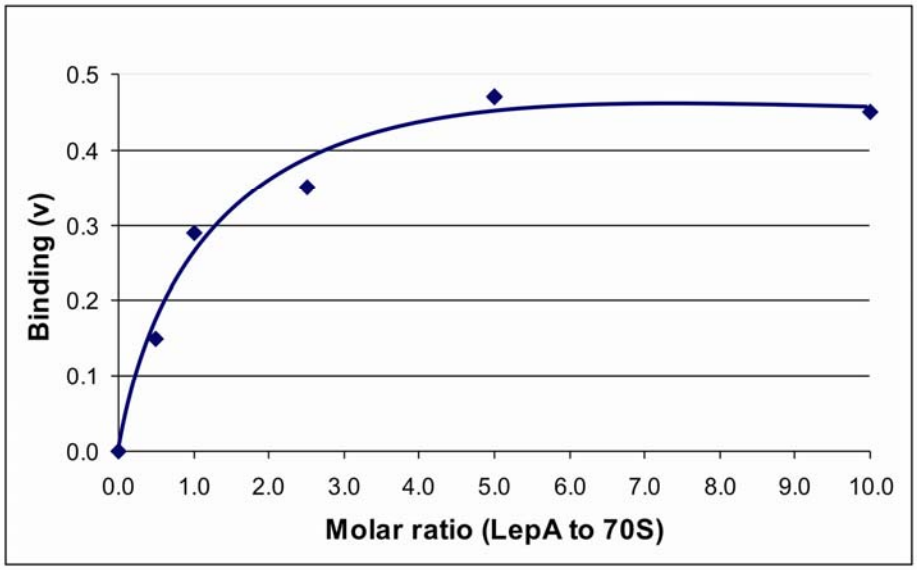

Figure 3.3.1.1_2 **Titration of LepA to *E. coli* re-associated 70S ribosome**

3.3.1.2 Competitive binding of LepA and EF-G to re-associated 70S

As a control we first test saturated binding of EF-G to re-associated 70S. At 2.5:1 of EF-G to 70S, the binding was saturated with occupancy of 50% (Figure 3.3.1.2_1).

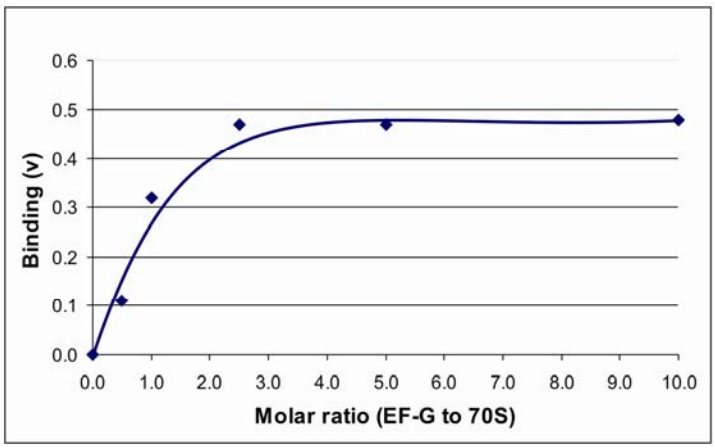

Figure 3.3.1.2_1 **Titration of EF-G to *E. coli* re-associated 70S ribosome**

Then the titration of LepA in the presence of EF-G (70S + 2.5 times EF-G) was preformed and the Figure 3.3.1.2_2 shows that there was no competition between LepA and EF-G binding onto re-associated 70S ribosome. This means that EF-G and LepA do bind to different conformer of the re-associated 70S ribosomes each present in a population of about 50%.

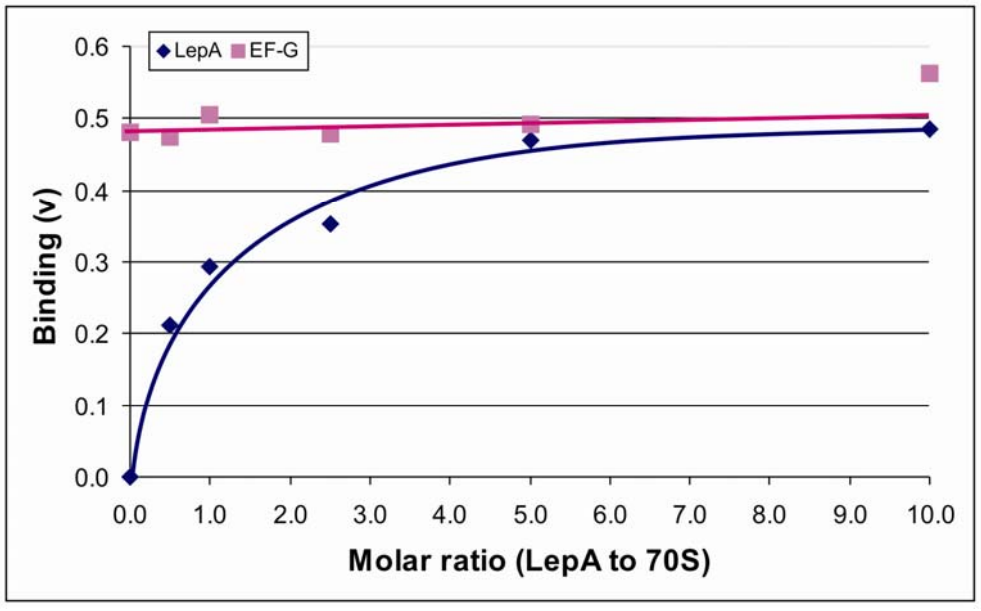

Figure 3.3.1.2_2 **Binding of LepA to 70S•EF-G**

3.3.1.3 Complex preparation for Cryo-EM

In the preceding section we saw that LepA does not compete with the binding of EF-G. Since the substrate for EF-G binding is the PRE state, this result suggests that LepA might target the POST state ribosomes. Therefore, complexes of different functional states of ribosome were prepared and the binding of LepA to them analyzed (Figure 3.3.1.3).

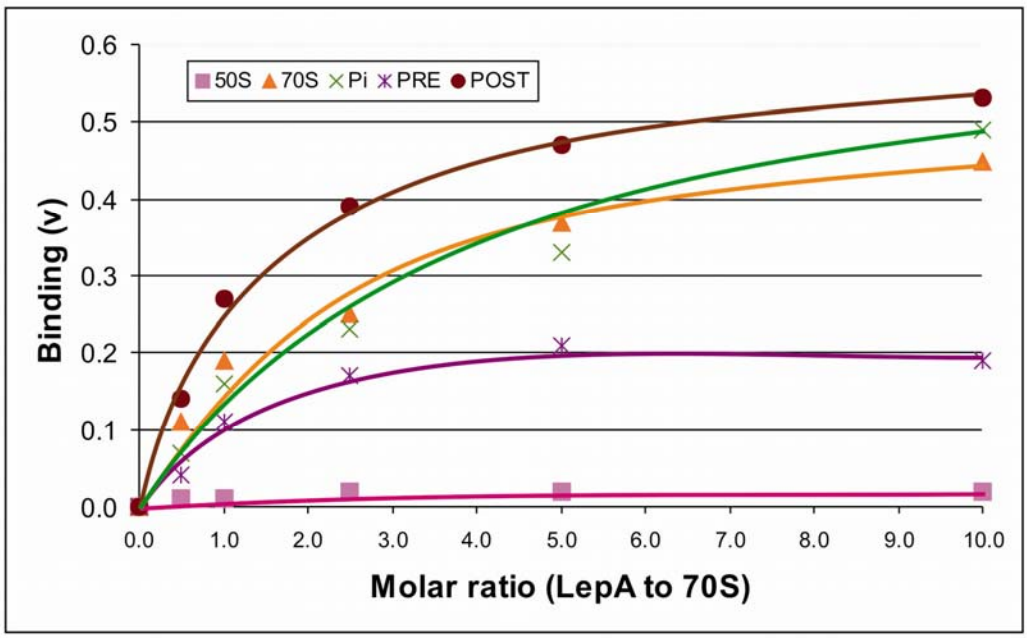

Figure 3.3.1.3 **Binding of LepA to ribosome or complexes**

The results showed that the POST complex has the highest affinity for LepA. By titration of LepA to POST complex, the disassociation constant of LepA to the POST and PRE complex were Kd = 0.252 x 10^{-6} M and Kd = 1.15 x 10^{-6} M, respectively.

3.3.1.4 Cryo-EM reconstruction of LepA•POST complex

The LepA•POST complex sample prepared in the last section was structurally analysized by Cyro-EM. Thanks to Dr. S. R. Connell, the reconstruction figure of this complex is primarily achieved (Figure 3.3.1.4).

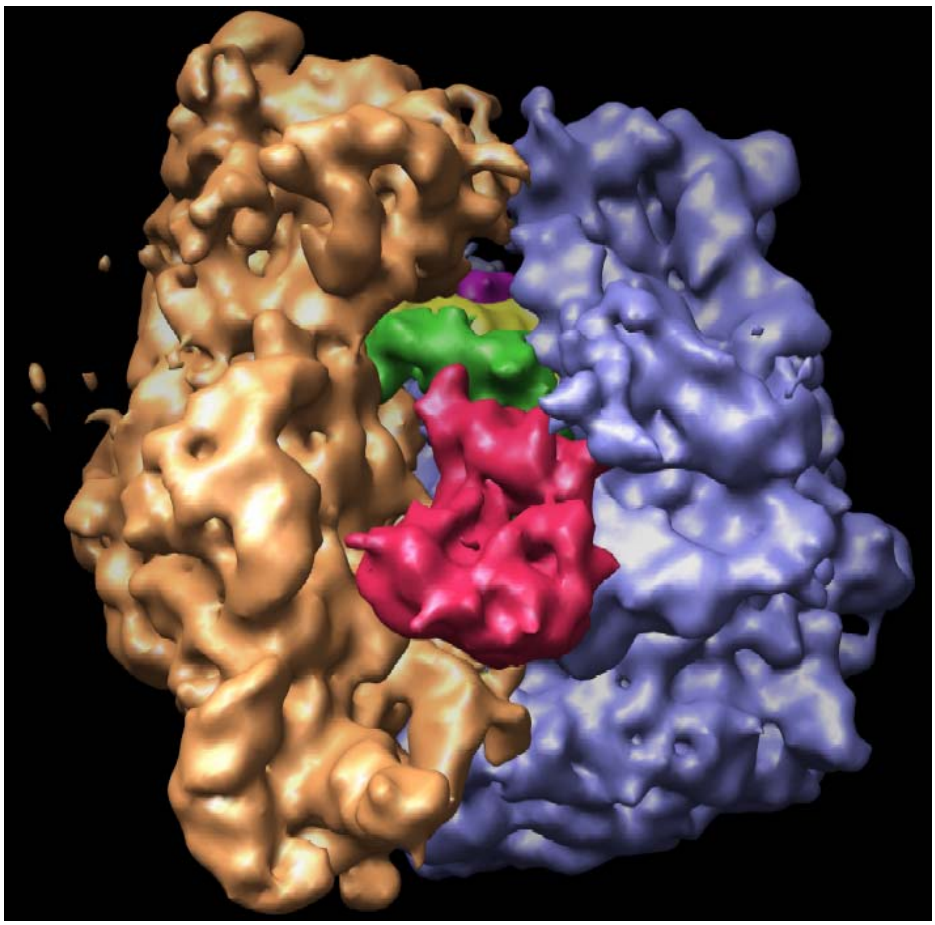

Figure 3.3.1.4 **Cryo-EM reconstruction of LepA•POST complex**
The complex is viewed from the L7/L12 stalk: 50S subunit in blue, 30S subunit in gold, LepA in red, A- P- and E-site tRNAs arein green, yellow and purple respectively.

In this reconstruction picture, it is clear that LepA (red) is located under the L7/L12 stalk and interacts mostly with the GTPase associated center as standard elongation factors, i.e. EF-G or ternary complex. But unlike EF-G, whose domain IV can go deeply in to the A-site, with binding of LepA the A-site tRNA (green) can correctly locate without any interruption.

3.3.2 GTPase assay of LepA

3.3.2.1 GTPase activity of LepA with re-associated 70S

The high similarity between the domain structure of LepA with that of EF-G prompted us to test the ribosome-dependent GTPase activity of LepA. EF-G is known to

have the strongest ribosome-dependent GTPase activity among all known G proteins involved in translation. When the ribosome stimulation of GTP cleavage is not coupled to protein synthesis, it is referred to as being uncoupled GTPase activity.

Figure 3.3.2.1 demonstrates that LepA not only exhibits an uncoupled GTPase activity, but that this activity is stimulated by re-associated ribosome at least to the same extent as that of EF-G.

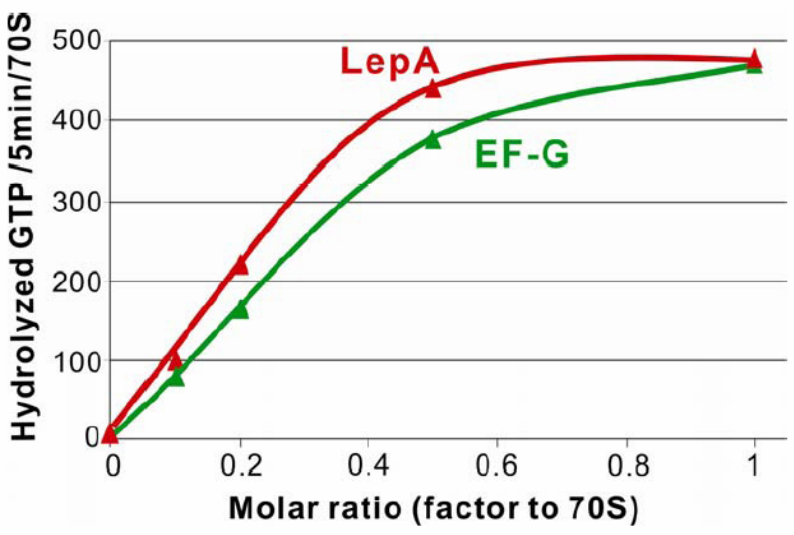

Figure 3.3.2.1 **Uncoupled GTPase activity of LepA compared to EF-G**

3.3.2.2 GTPase activity with ribosome complexes in functional states

Here we asked the same question as in the binding assay: Does LepA react mostly with the PRE or the POST state of the ribosome?

Re-associated ribosomes programmed with mRNA, bound with decoding tRNAs formed Pi, PRE and POST (2.7.2) complexes. LepA incubated with each complex showed distinct GTPase activity (Figure 3.3.2.2).

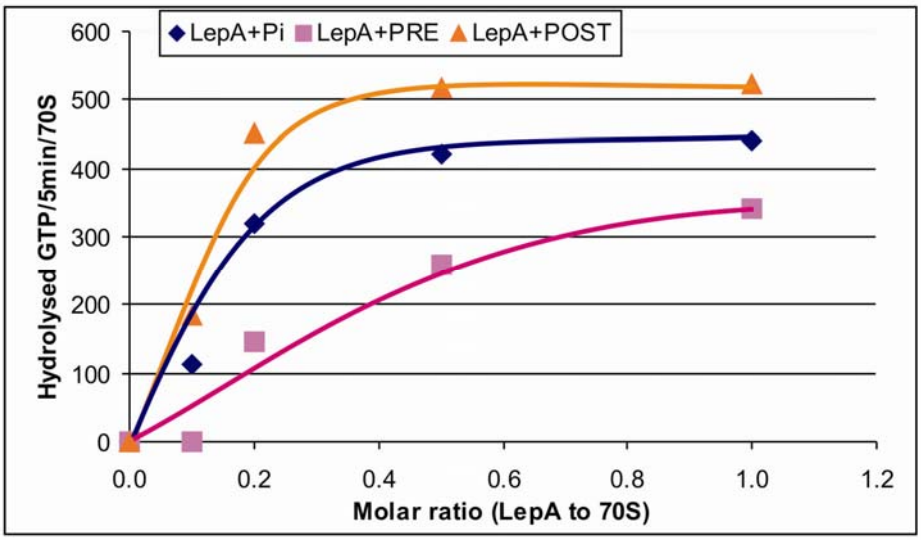

Figure 3.3.2.2 **GTPase activity of LepA with different ribosome complex**

During the initial phase of each curve indicates that the POST state activates LepA dependent GTPase most efficient, whereas the PRE state was the worst activator. The slopes of Pi, PRE and POST curve during this phase, namely 0.1-0.2 x LepA/70S indicate the following turnover numbers (GTP's cleaved per 1 LepA in 5 min): 1500, 700 and 2250, respectively. It follows that the strongest activation ability is seen with the POST state, the Pi state reaches ~2/3 of this value and PRE is ~1/3.

3.3.3 LepA's effect on puromycin activity of Pi or POST complex

Puromycin, an analogue of the 3'-end of an aminoacyl-tRNA that binds to the A-site region of the peptidyltransferase centre, reacts with the P-site binding peptidyl-tRNA (Figure 3.3.3_1). It follows that the Pi and POST states, in which A-site is free, the puromycin reaction is positive. But when A-site is occupied, e.g. in the PRE state, the puromycin reaction cannot occur.

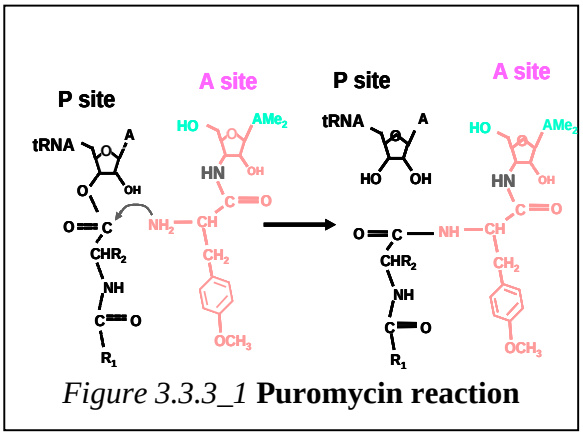

Figure 3.3.3_1 **Puromycin reaction**

Puromycin reaction of Pi or POST complex with/without LepA was checked. Surprisingly, in the presence of LepA the POST state did not react with puromycin any

more, whereas the Pi state still did (Figure 3.3.3_2). At the same time LepA did not affect the amount of tRNAs bound to the programmed ribosomes.

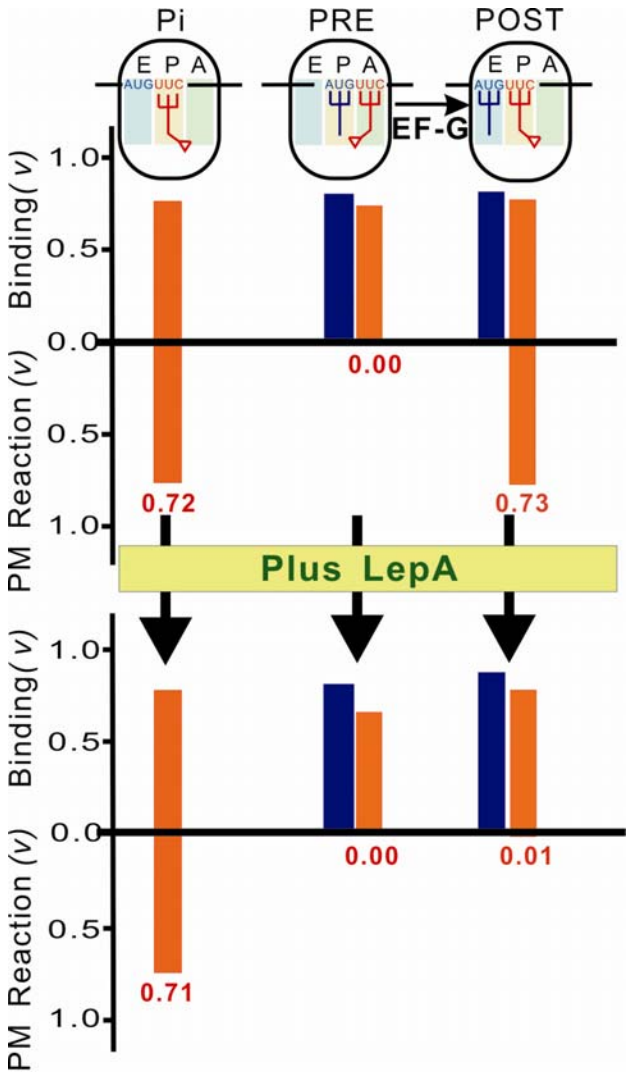

Figure 3.3.3_2 **tRNA binding and puromycin reaction of different state ribosome complexes before and after an incubation with LepA•GTP**

Figure 3.3.3_3 shows an additional detail. In the presence of GTP LepA works catalytically in a similar fashion as EF-G: the LepA•GTP effect saturates at 0.4 molecules per 70S ribosome; the corresponding number for EF-G is 0.3. However, in the presence of the non-hydrolysable GTP analog GDPNP, the LepA action becomes stoichiometric, saturating at about 1 molecule per 70S ribosomes. In analogy to GTP we

conclude that GTP cleavage is required for dissociation of LepA from the ribosome and thus the factor behaves like a typical G protein (reviewed by (Bourne, 1991)).

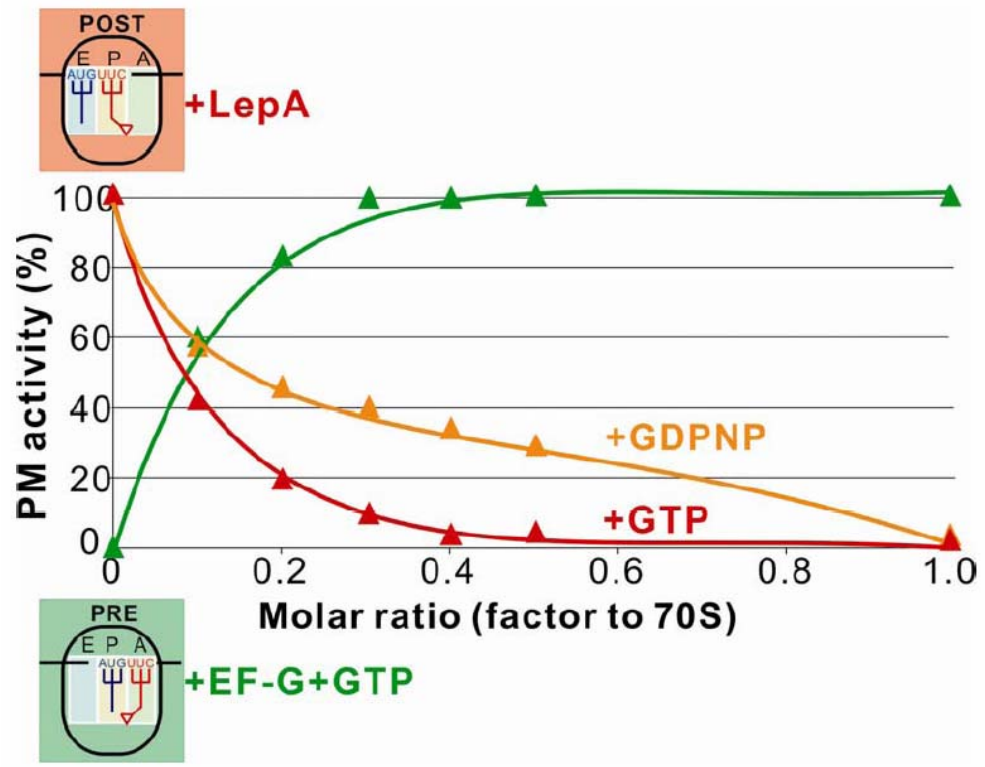

Figure 3.3.3_3 **Puromycin assay of LepA•GTP/GDPNP or EF-G•GTP titration to POST or PRE complex**

3.3.4 Dipeptide formation analysis in the presence of LepA

Dipeptide formation employing genuine aa-tRNA as acceptor is more robust than the puromycin reaction, *viz*. dipeptides can still be formed efficiently even when puromycin can no longer react with a peptidyl-residue at the P site region of the peptidyltransferase centre (Youngman et al., 2004). Therefore, we tested dipeptide formation with Pi and POST states, both of which carried an Ac[^{14}C]Phe-tRNA at the P site and in the case of the POST state an additional deacylated tRNA$_f^{Met}$ at the E site. In both cases, dipeptides were efficiently formed upon addition of [^{3}H]Lys-tRNA^{Lys}•EF-

Tu•GTP (Figure 3.3.4, arrow). In striking contrast, the POST state showed no traces of dipeptides in the presence of LepA•GTP, whereas dipeptide

formation of the Pi state remained unaffected, in agreement with the results obtained from the puromycin reaction above.

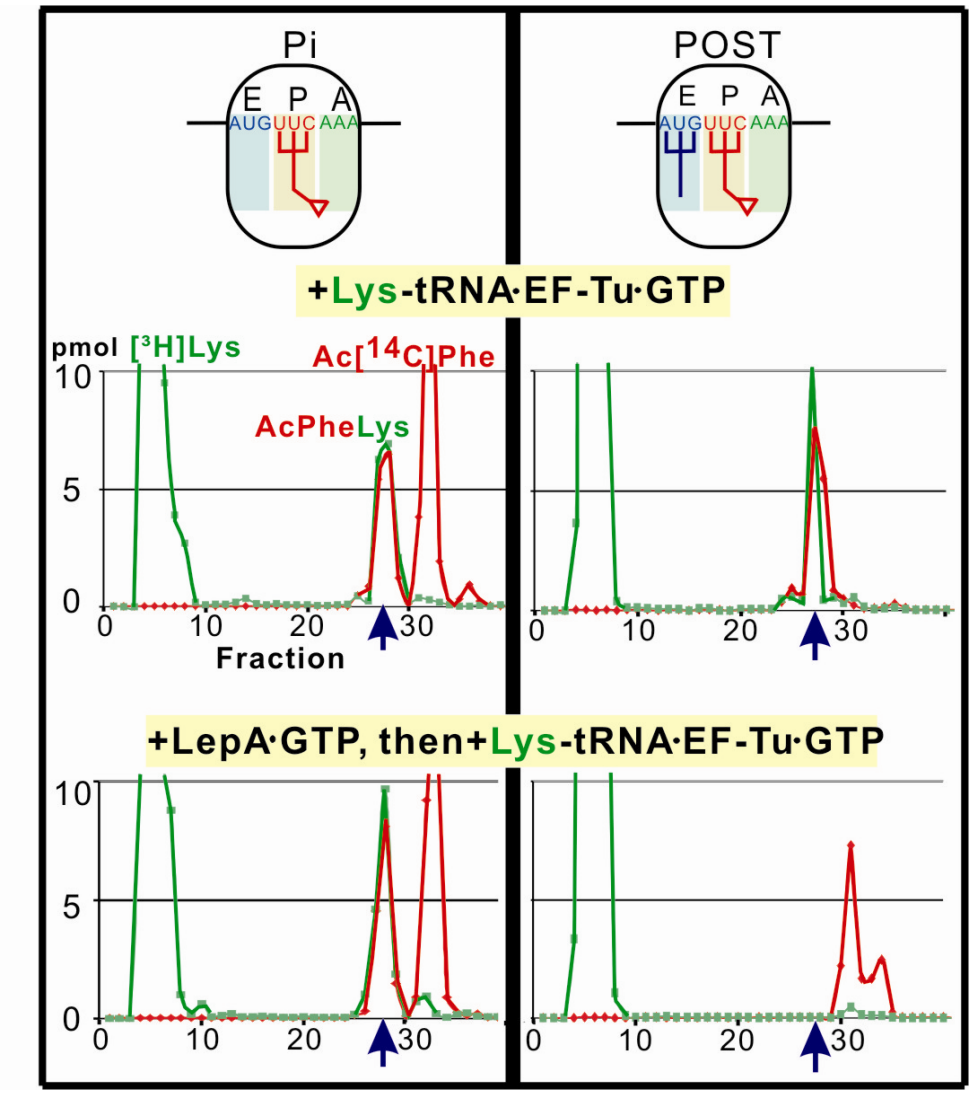

Figure 3.3.4 **Dipeptide bond formation of Pi and POST complex without/with LepA**

3.3.5 LepA is a "back-translocator"?

A possible explanation for the unexpected behavior of the POST complex in the presence of LepA is that this factor induces a "back-translocation" of the POST state to the PRE state, since the occupation of the A site by the AcPhe-tRNA after back-translocation would prevent the puromycin reaction or binding of a cognate ternary complex to the A site. In contrast, the Pi state cannot be back-translocated, since an A site cannot be occupied in a stable fashion without a tRNA in the adjacent P site (Rheinberger et al., 1981). To test this hypothesis we employed two strategies:

(i) Footprint assay:

a) Chemical probing of the tRNA positions through analysis of diagnostic base protections in the 16S rRNA;

b) Monitoring a POST state-specific 23S rRNA conformation marker by Pb^{2+} cleavage,

(ii) A direct test of the ribosome movement on the mRNA with the toeprint assay.

3.3.5.1 Footprint assay monitoring tRNA protection pattern

A-site bound tRNAs protect a set of characteristic bases in the 16S and 23S rRNA from chemical modifications (Moazed and Noller, 1989a; Moazed and Noller, 1990). In order to unravel the ribosomal location of AcPhe-tRNA in our various complexes, we screened two known A-site tRNA footprints in 16S rRNA. At position A1408 in the decoding center, AcPhe-tRNA in the PRE state ribosome produced the expected A-site footprint, which however was lost upon translocation to the P-site in the POST state (Figure 3.3.5.1_A). Significantly, the addition of LepA•GTP to the POST state re-established the protection at A1408. An essentially identical tRNA footprinting pattern was observed at position U531 of 16S rRNA (Figure 3.3.5.1_B). These data are compatible with the notion that AcPhe-tRNA re-occupies the A-site upon LepA addition to POST state ribosomes.

Furthermore, also the 50S subunit shows structural evidence for a LepA-promoted back-translocation. Previously we showed that the 50S conformation of the post-translocational ribosome is different to that of the pre-translocational ribosome - a difference that could be monitored by site-specific Pb^{2+} cleavage of 23S rRNA (Polacek

et al., 2000). A diagnostic cleavage was detected at position C2347, which was significantly enhanced in the POST compared to the PRE state. Figure 3.3.5.1_C demonstrates that LepA brings the strong signal observed in the POST state down to the level of the PRE signal suggesting that upon binding of LepA•GTP, the ribosome adopts a PRE configuration.

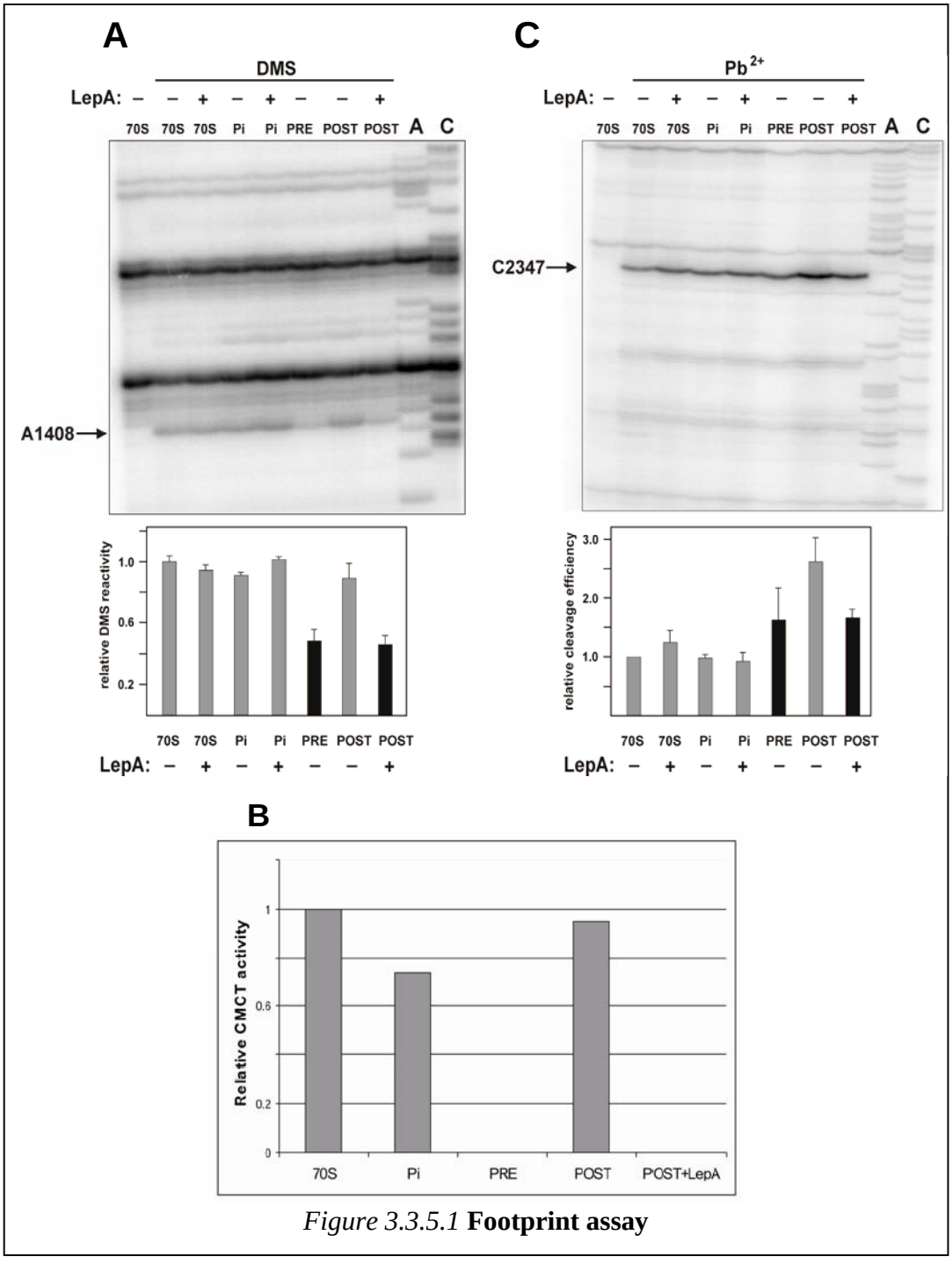

Figure 3.3.5.1 **Footprint assay**

3.3.5.2 Toeprint assay monitoring mRNA movement

Additionally, the back-translocation ability of LepA was tested using the toeprinting assay. In this assay, the programming mRNA carries a complementary [^{32}P]-labeled DNA primer at the 3' end located downstream of the ribosome. The primer is prolonged by reverse transcription until the polymerase clashes with the ribosome. Thus, the length of the transcript indicates the distance between the primer and the ribosome, which becomes shorter by three nucleotides following translocation (Hartz et al., 1990) and therefore should be longer after the putative back-translocation. Controls indicate the expected length of the transcripts, when either of two adjacent codons were alternatively located at the P site by corresponding tRNA binding to the P site. A translocation of a PRE state shows a shortage of the reverse transcript by three nucleotides, while the addition of LepA•GTP to a POST state prolongs the transcript again proving that LepA is a back-translocator (Figure 3.3.5.2).

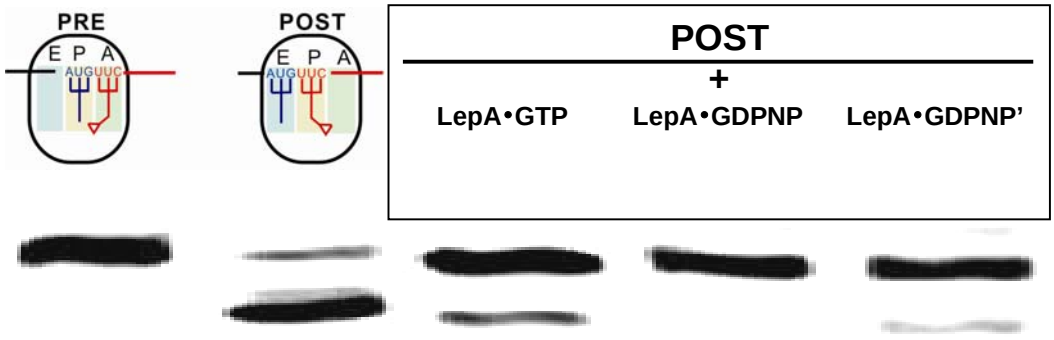

99.9%	17.8%	77.1%	98.5%	76.3%
0.1%	82.2%	22.9%	1.5%	23.7%

Summary of the proportion of the two bands from each sample, the upper band stands for the mRNA location of the PRE state and the lower for the POST.

Figure 3.3.5.2 **Toeprint assay**

The difference between sample 5 and sample 4 is the condition of reverse transcription, namely the Mg^{2+} concentration increased from 4.5 mM to 15 mM according to (Youngman et al., 2004). The results show that our 4.5 mM standard condition is more optimal.

3.4 Effects of LepA on accuracy of protein in vitro *synthesis*

3.4.1 LepA optimizing protein synthesis

We have demonstrated previously that bacterial coupled transcription-translation systems (e.g. RTS, Roche) can produce large amounts of protein (e.g. 4 mg/ml GFP, green fluorescent protein), but under standard conditions (30°C incubation) the active fraction is unsatisfactorily low (50±20%; (Dinos et al., 2004)). Since LepA is an elongation factor with back-translocation ability, it was interesting to study its effect on protein synthesis in such a coupled system.

3.4.1.1 RTS system: GFP and luciferase synthesis

The experimental set-up is that the total protein amount is assessed *via* SDS-PAGE, since the reporter protein GFP does not overlap in a Coomassie stained gel with any other protein present in the cell lysate. This enables the GFP band to be scanned and the total amount accurately determined by comparison to a reference GTP added to the same gel. In parallel, the same samples are loaded onto native gels and the active amount is revealed *via* the fluorescence of the GFP band. Figure 3.4.1.1_1 shows that in the presence of increasing amounts LepA, the total GFP amount increases, when 0.1 molecules LepA are added per 70S. Further addition of LepA leads to a rapid reduction in the GFP production, eventually blocking completely the total synthesis at a molar ratio

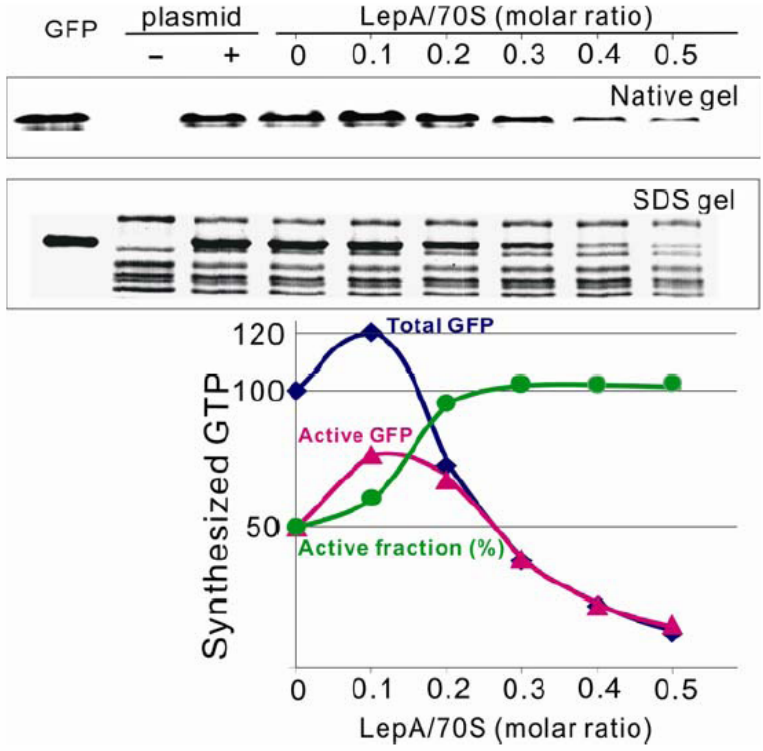

Figure 3.4.1.1_1 **Effect of LepA onto GFP synthesis in RTS system**

of lepA:70S = 1:1, in agreement with the toxic effects of overproduced LepA *in vivo* seen in Figure 3.2.1.2. In contrast, the native gel reveals that the active GFP amount increases to attain the same levels as the total GFP amount at LepA stoichiometries of ≥0.2 LepA per 70S. In other words, addition of LepA promotes the synthesis of fully active proteins.

A similar analysis was performed with a second unrelated protein, the luciferase. In this case, the total amount was monitored by a sequencing SDS-PAGE stained with silver staining, and the active amount was assessed by the enzyme activity compared with commercially available 100% active luciferase. Figure 3.4.1.1_2 shows that LepA behaved in the way same as seen with the GFP synthesis.

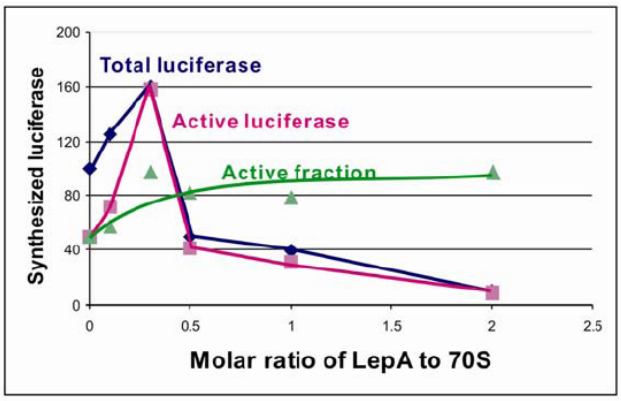

Figure 3.4.1.1_2 **Effect of LepA onto luciferase**

Figure 3.4.1.1_3 summarizes the beneficial effects LepA has on the protein synthesis in a coupled transcrip-tion-translation system in the presence of 0.3 molecules per 70A ribosome.

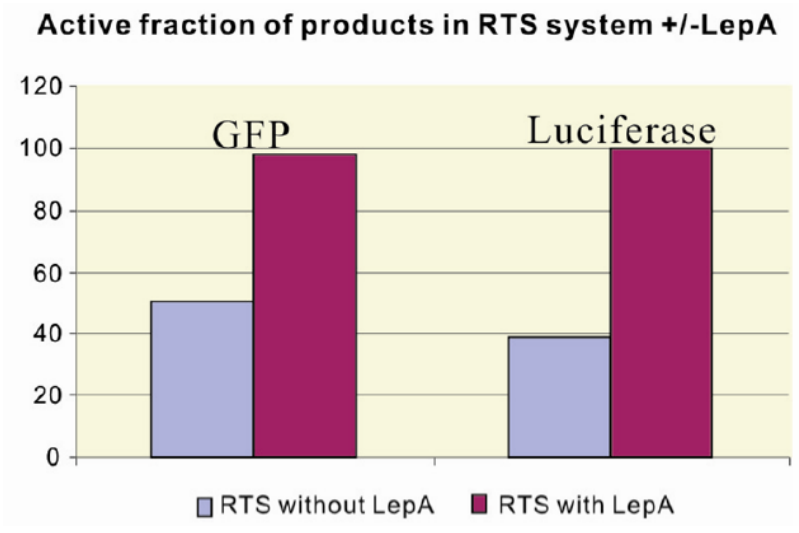

Figure 3.4.1.1_3 **Effects of LepA on RTS system**

We conclude that LepA can not only increase the total protein yield but more importantly improves the accuracy of protein synthesis to enable the synthesis of fully active proteins.

3.4.1.2 Promega system: GFP synthesis

Furthermore, another commercial *in vitro* protein biosynthesis was checked as well. Figure 3.4.1.2 shows the GFP synthesis in Promega system. Until up to 10 x LepA pro ribosome, the active fraction increased only slightly. The reason probably was that the efficiency of the system was only marginal as compared with the Roche system (~70 μg/ml as compared to ~500 μg/ml). This means that for unknown reasons the Promega system works near the background level, and the factor responsible for the low efficiency might be also responsible for the negligibly low active fraction of about 15%.

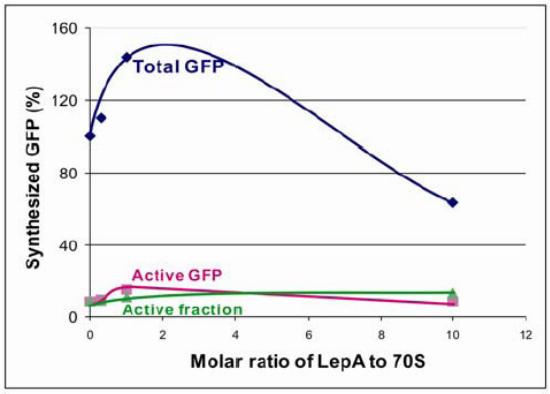

Figure 3.4.1.2 **LepA effects on Promega**

3.4.2 LepA's function in the presence of antibiotics

We have reported before (Dinos et al., 2004) RTS is a powerful system to determine some parameters of the mechanism of antibiotics. By knowing the total synthesis and the active fraction of GFP in the presence of antibiotics, the fidelity of protein synthesis is monitored using a natural mRNA (GFP) and no radioactive amino acids.

3.4.2.1 Aminoglycosides

The best-known drugs that induce mis-incorporations are aminoglycosides, such as paromomycin, which binds directly at the decoding center and impairs the tRNA selection process (Ogle et al., 2001). Since LepA was shown to enhance the fidelity of translation, we asked the question as to whether LepA can also correct paromomycin induced translational errors? Figure 3.4.2.1_1, left panel, demonstrates that the paromomycin severely decreases GFP synthesis, blocking it completely at 2 μM concentration. On the native gel, the fluorescence of GFP was strongly reduced by paromomycin addition, indicating that paromomycin causes a drop in the active GFP

fraction. In the presence of LepA, a similar paromomycin-dependent reduction in the active GFP fraction is observed (Figure 3.4.2.1_1, right panel) indicating that LepA cannot counteract the paromomycin-induced errors. Equivalent results were obtained with other aminoglycosides, such as streptomycin and viomycin (Figure 3.4.2.1_2) that also bind to the decoding center of the A site.

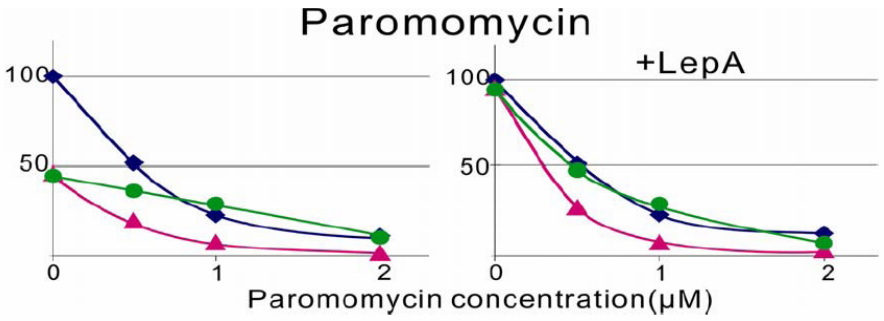

Figure 3.4.2.1_1 **LepA effect on GFP synthesis in the presence of paromomycin**

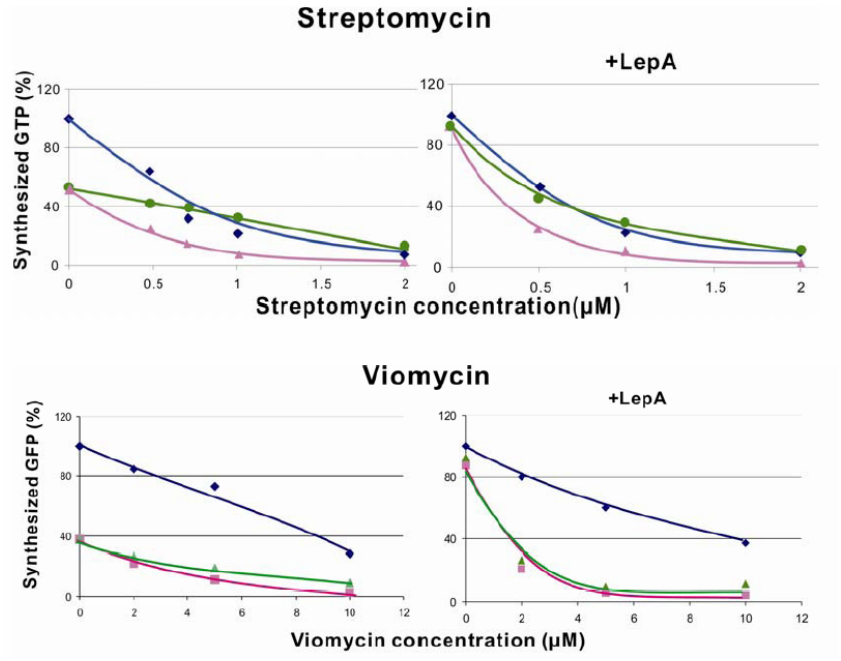

Figure 3.4.2.1_2 **LepA effect on GFP synthesis in the presence of streptomycin and viomycin**

3.4.2.2 Edeine

Edeine is a drug the inhibition mechanism was only recently unraveled by our group (Dinos et al., 2004). Edein binds within the E site. In the presence of LepA, the damage from the drug wasn't rescued either (Figure 3.4.2.2).

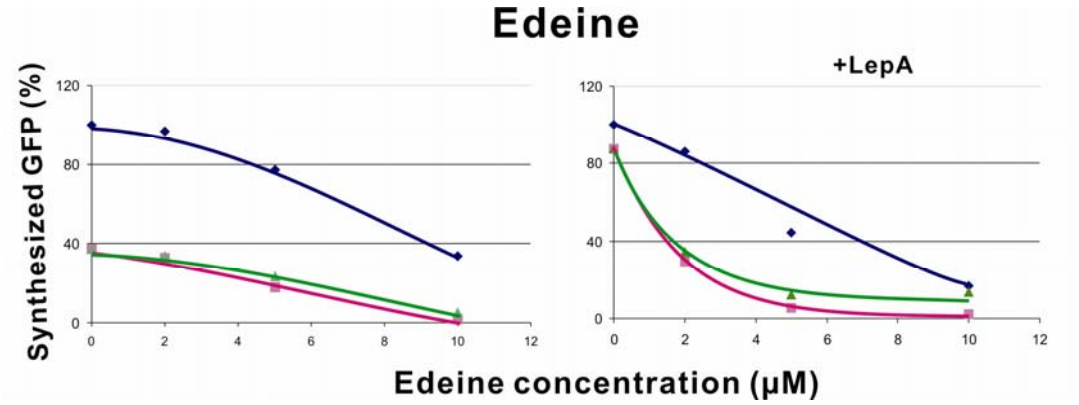

Figure 3.4.2.2 **LepA effect on GFP synthesis in the presence of edeine**

3.4.3 LepA's function in the presence of Mg^{2+}

Coming back to the high ionic stress problem: The fidelity of protein synthesis is very sensitive to changes in magnesium concentration, such that an increase of only 5 mM (from 12 to 17 mM) reduced the total synthesis of GFP down to 40% and the active fraction down from 50% to 25% (Figure 3.4.3, left panel). Addition of LepA dramatically altered the picture: with a Mg^{2+} increase up to 3 mM the total synthesis was not reduced, in fact a small but significant increase is observed (120%) and the active fraction is maintained at ~100%. It follows that the dominant effect of LepA was seen at a Mg^{2+} increase of 2-3 mM, where lepA doubled the total protein synthesis with an active fraction of virtually 100%.

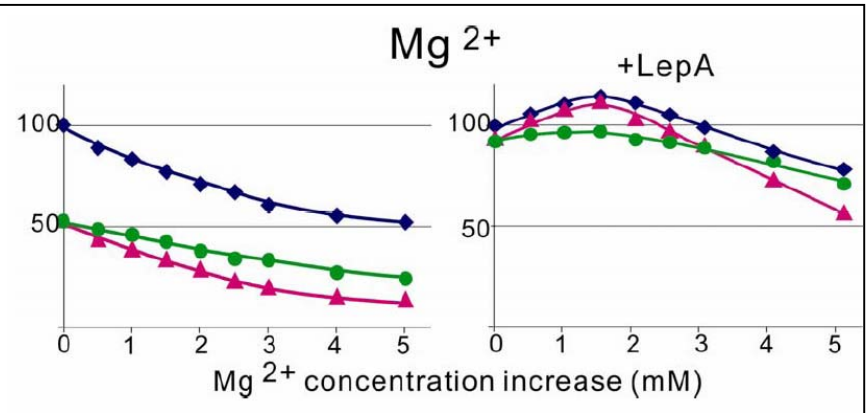

Figure 3.4.3 **LepA effect on GFP synthesis with increase Mg^{2+} concentration**

3.5 Appendix

3.5.1 Extended phylogenetic LepA

An extended evolution tree on a large set of organisms (Figure 3.5.1) was calculated compared to the tree shown before (Figure 3.1_1). The essentials of the

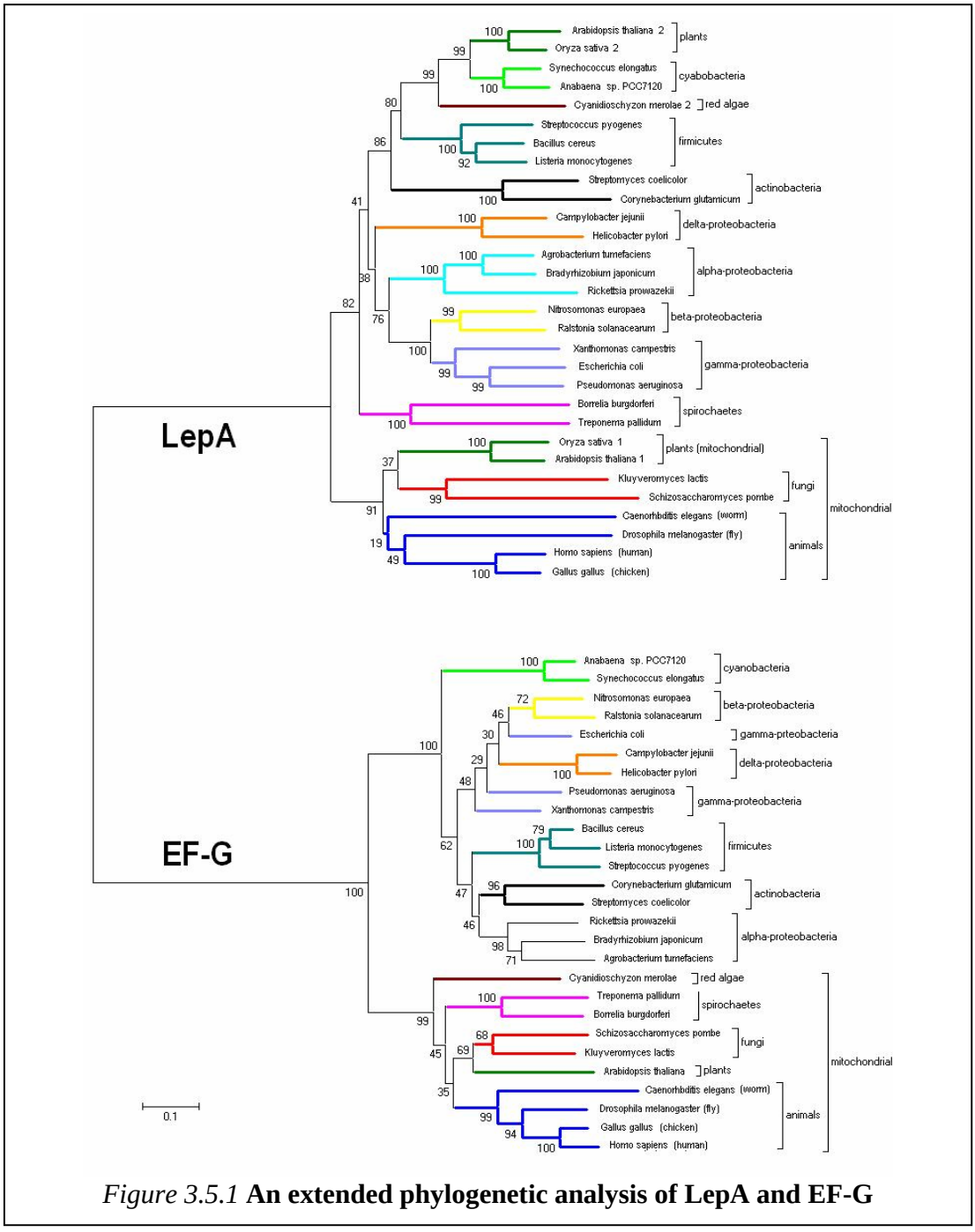

Figure 3.5.1 **An extended phylogenetic analysis of LepA and EF-G**

phylogenetic tree already emerged during the analysis of the smaller data set. Due to the higher number of taxa the second data set offers an enhanced resolution of internal branching patterns in the bacterial subtree and confirms results from the first data set.

3.5.2 Studies with the Elongation Factor EF-P

3.5.2.1 EF-P *in vivo* distribution

A side project dealt with the function of elongation factor P (EF-P). EF-P was found as a protein that stimulates the peptidyltransferase activity of the 70S ribosome in *Escherichia coli* (Ganoza and Barraclough, 1975). EF-P enhances dipeptide synthesis with *N*-formylmethionyl-tRNA and puromycin *in vitro*, suggesting its involvement in the formation of the first peptide bond of a protein (Ganoza, 1977). However, one has to say that these and other effects were ascribed to EF-P, none of which gave a convincing picture of EF-P functions (Aoki et al., 1997).

Recently the crystal structure of EF-P (*T. thermophilus)* was achieved showing that it has mimicry of tRNA (Figure 3.5.2.1_1, (Hanawa-Suetsugu et al., 2004)).

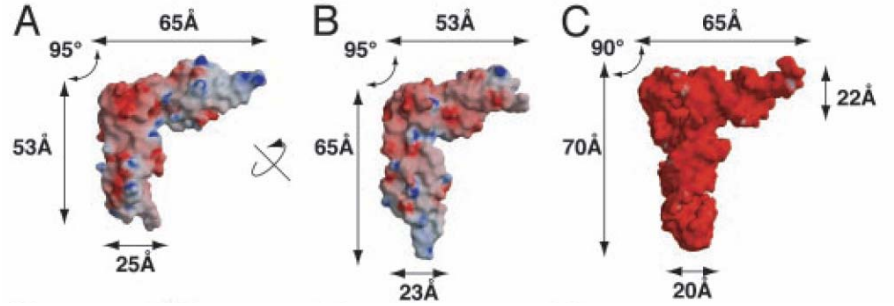

Figure. 3.5.2.1_1 **Structure comparison of EF-P with tRNA**
(A , B) EF-P from *T. thermophilus*. (C) $tRNA^{Phe}$ from *S. cerevisiae*.

The EF-P homologue in eukarya and archaea is eukaryotic initiation factor 5A (eIF-5A) which has domains corresponding to domains I and II of EF-P (Figure 3.5.2.1_2, (Hanawa-Suetsugu et al., 2004)). The factor eIF-5A is not essential in yeast (Kang and Hershey, 1994) and its function is still unknown.

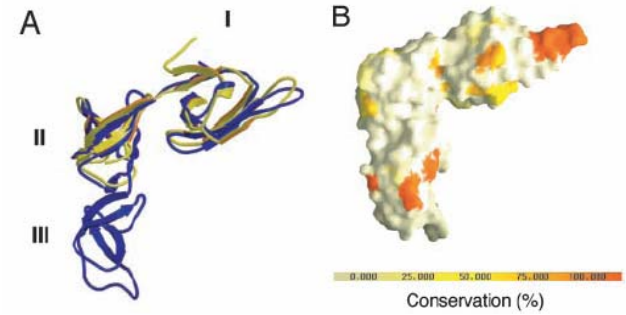

Fig. 3.5.2.1_2 **Structure comparison of EF-P and eIF-5A**
(*A*) Superimposition of the ribbon diagrams of *T. thermophilus* EF-P (blue) and *M. jannaschii* eIF-5A(yellow). (*B*) Amino acid residues conserved in EF-Ps and eIF-5As color-coded on the surface of *T. thermophilus* EF-P.

Since all the experimental results and the EF-P structure indicated that it should function in connection with the ribosome, the question concerning its interaction with the ribosome is of great interest. For structural analysis of EF-P • 70S complex, first I checked the EF-P *in vivo* distribution associated with ribosomes.

A lysate (S30 fraction) of cells that overexpressed EF-P was prepared (2.3.9) and ribosomal subunits, monomer and polymer were separated on a sucrose gradient in an SW40 rotor (Figure 3.5.2.1_3, red curve). The gradient was collected in small fractions so that each type of ribosome or subunits could be separated from each other (each white column in the table stands for one collection fraction). Later on, the EF-P in each fraction was checked by anti-EF-P antibody (Figure 3.5.2.1_3, "Anti-EF-P" lane on the bottom).

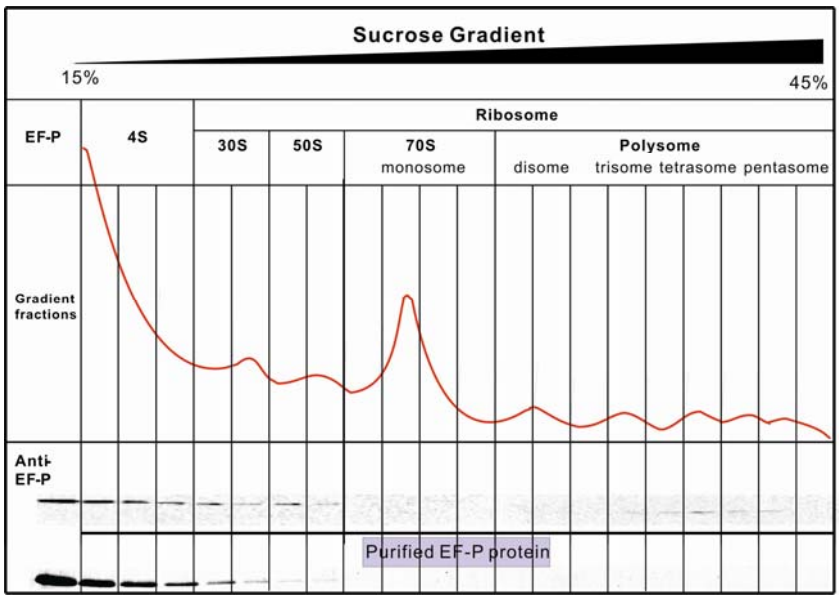

Figure 3.5.2.1_3 **Western Blot of EF-P distribution in S30**

The result shows that EF-P

migrated together with 30S, 50S ribosomal subunits and polysomes from trisomes to pentasomes. Because this S30 preparation contained overexpressed EF-P, most of the EF-P is expected to be present in the protein region (4S) of the gradient. As a control purified EF-P was subjected to a corresponding gradient and Western blot analysis demonstrated that EF-P migrated in the 4S region and smears out a little into the 30S region (see second line of Anti-EF-P in Figure 3.5.2.1_3). We conclude that EF-P co-migrates essentially with the polysomes.

3.5.2.2 Preparation of EF-P ribosome complex for Cryo-EM

Since EF-P was found to co-migrate with ribosomes (mostly polysomes), the binding of EF-P with ribosomal subunits or re-associated 70S complex was checked. We could not observe any detectable binding under standard conditions (4.5 mM Mg^{2+} plus polyamines). When the Mg^{2+} concentration was changed from 4.5 to 10mM, two molecules EF-P per 70S were found (Figure 3.5.2.2), Kd = 0.24 x 10^{-6} M and Ka = 4.2 x 10^{6} M^{-1}.

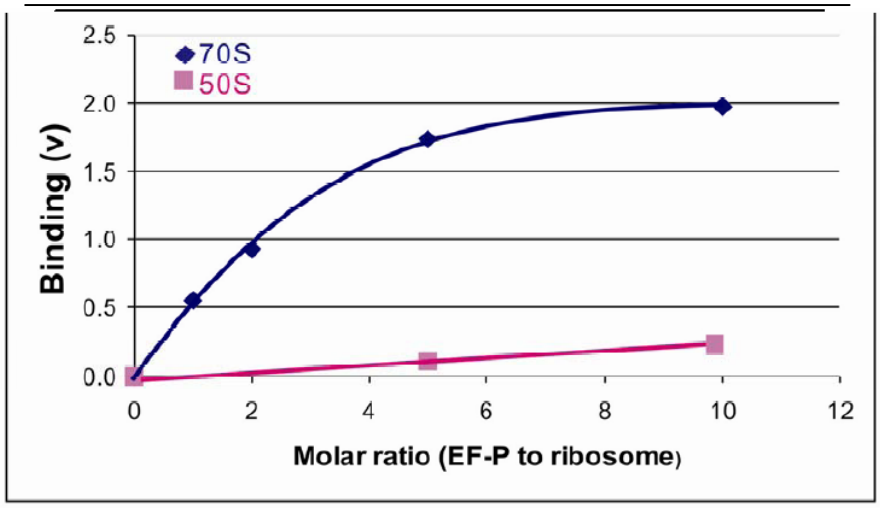

Figure 3.5.2.2 **Titration of EF-P to 70S**

3.5.3 Studies concerning the L7/L12 stalk

3.5.3.1 Binding of EF-G to *E. coli* 70S minus L7/L12

Large ribosomal subunit proteins L7/L12 are involved in forming the GTPase associated center which triggers the GTP hydrolysis on the elongation factors (EF) EF-G and EF-Tu. L7/L12 is the only protein present in four copies per ribosome, and the individual proteins bind tightly to each other to form two dimers being the main component of the L7/L12 stalk of the large ribosomal subunit. The NTDs of this tetramer bind to protein L10 and represent a fixed root of the stalk. In contrast, the CTDs are very flexible (Bocharov et al., 2004) and might help the release of the EFs (Hagiya et al., 2005). According to this hypothesis, 70S minus L7/L12 should still be able to bind an elongation factor. Figure 3.5.3.1 shows that the most EF-G binding was in GDP form on the incomplete 70S. The binding ratio (v) was quantified that in the cases of 70S+EF-G•GDP, 70S+EF-G•GTP and 70S*+EF-G•GTP are all 0.05 while in the case of 70S*+EF-G•GDP it is 0.25.

1	2	3	4	5	6	7	8	9	10	11	12
70S	70S *	70S+EF-G •GDP		70S+EF-G• GTP		70S*+EF-G •GDP		70S*+EF-G •GTP		EF-G	
		Su	Pe	Su	Pe	Su	Pe	Su	Pe	Su	Pe

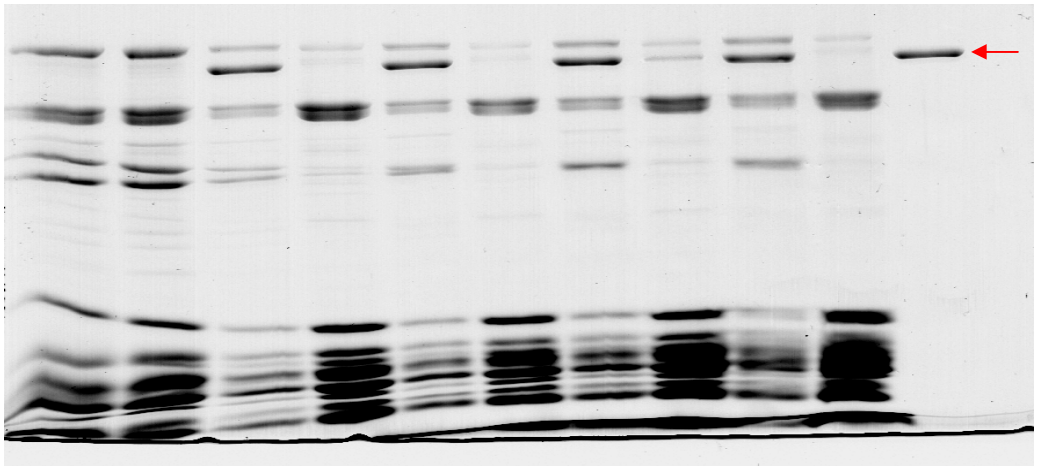

Figure3.5.3.1 **Binding of EF-G to 70S**
E. coli EF-G (red arrow) in GDP or GTP form was incubated with complete *E. coli* 70S or 70S without L7/L12 (70S*). After incubation the mix was purified through sucrose cushion to get supernatant (Su) and pellet (Pe).

3.5.3.2 Puromycin activity monitoring the EF-G dependent translocation of the PRE complex in the presence and absence of L7/L12

The *in vivo* molar ratio of EF-G to 70S is 0.3 to 1 so that EF-G triggers the tRNAs' translocation catalytically. But if L7/L12 is involved in the turn over of the elongation factors, the absence of the L7/L12 should change the EF-G effect from a catalytic mode to a stoichiometric mode of action. Figure 3.5.3.2 shows indeed that puromycin activity of EF-G was saturated to complete 70S PRE complex at 0.3 x while to the minus L7/L12 complex EF-G was needed 1:1 ratio to ribosome to translocate the tRNAs completely. This finding is consitent with the hypothesis that L7/L12 is invovlved in the turn over of the EFs, but could be also explained that the affinity for EF-G is reduced by a factor of below 5, if - as generally believed – the L7/L12 is an important component of the EFs' binding site.

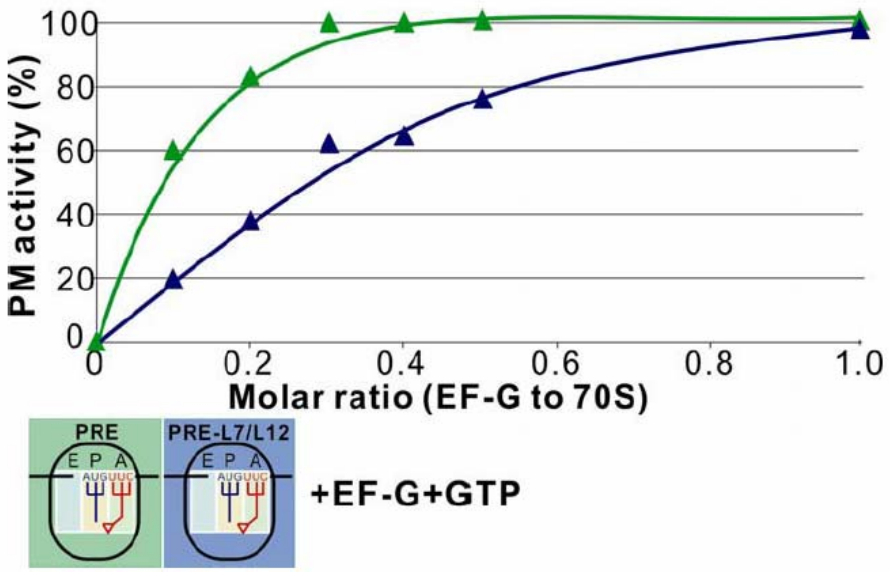

Figure 3.5.3.2 ***PM activity of EF-G titration to PRE complex or PRE minus L7/L12***

3.5.4 Effect of the Shine-Dalgarno sequence on the first dipeptide formation

The E-site tRNA is responsible for maintaining the reading frame during protein synthesis (Marquez et al., 2004) and for an accurate selection of the cognate aa-tRNA at the A site, in particular for the discrimination against the non-cognate aa-tRNAs ((Geigenmüller and Nierhaus, 1990); for review see (Nierhaus, 1993)). The only aa-tRNA selection without an occupied E site occurs at the first A-site occupation just after initiation, where only the P site is filled with the initiator tRNA leaving the E site free. Therefore, the first aminoacyl-tRNA selection after initiation should be highly error prone, what has, however, never been observed. One possibility of solving this accuracy problem might be an of the Shine-Dalgarno (SD) interaction with the 3'-end of the 16S rRNA of the small ribosomal subunit, that might functionally replace the lacking codon-anticodon interaction at the E site. We could verify this hypothesis: Figure 3.5.4_1 shows that in the presence of an SD sequence (for the mRNA sequence see 2.5.1.5) the selection of the aa-tRNA at the A site perfectly discriminates against non-cognate aa-tRNAs, whereas in the absence of a SD sequence a significant dipeptide with the non-cognate Asp-tRNA (codon at the A site is GUA for Val-tRNA and it is a non-cognate codon for Asp-tRNA GAU/C) is formed. The red arrow shows the location of the f[^{3}H]Met-[^{3}H]Asp dipeptide. Because the non-cognate [^{3}H]Asp-tRNA was labeled extremely hot so that even little amount of f[^{3}H]Met-[^{3}H]Asp dipeptide could be easily detected, i.e. 12700 cpm [^{3}H] in the elution fraction 25 was detected which belonged to the ideal region for counting. In comparison that in the left panel the elution fraction 25 was only 906 cpm detected. The cpm of the fraction 20-30 were zoomed in and shown in the lower panel of Figure 3.5.4.

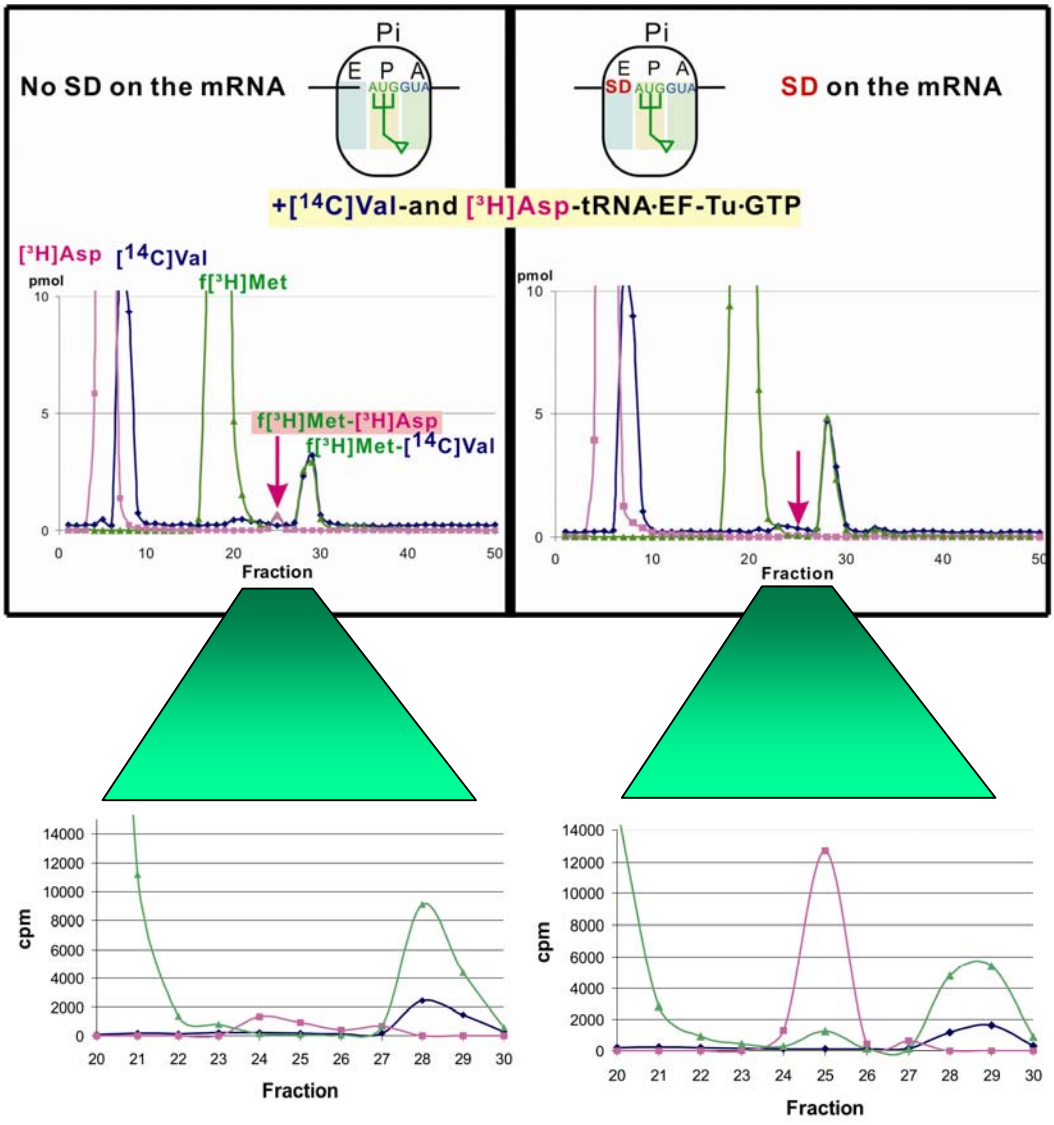

Figure 3.5.4 Effect **of SD sequence on first dipeptide formation**